PHYSICAL REVIEW D **91,** 095010 (2015)

Dark matter and gauge coupling unification in nonsupersymmetric SO(10) grand unified models

Yann Mambrini,[1] Natsumi Nagata,[2,3] Keith A. Olive,[2] Jérémie Quevillon,[4] and Jiaming Zheng[2]

[1]*Laboratoire de Physique Théorique Université Paris-Sud, F-91405 Orsay, France*

[2]*William I. Fine Theoretical Physics Institute, School of Physics and Astronomy, University of Minnesota, Minneapolis, Minnesota 55455, USA*

[3]*Kavli Institute for the Physics and Mathematics of the Universe (WPI), The University of Tokyo Institutes for Advanced Study, The University of Tokyo, Kashiwa, Chiba 277-8583, Japan*

[4]*Theoretical Particle Physics & Cosmology, Department of Physics, King's College London, London WC2R 2LS, United Kingdom*

(Received 3 March 2015; published 13 May 2015)

Unlike minimal SU(5), SO(10) provides a straightforward path towards gauge coupling unification by modifying the renormalization group evolution of the gauge couplings above some intermediate scale which may also be related to the seesaw mechanism for neutrino masses. Unification can be achieved for several different choices of the intermediate gauge group below the SO(10) breaking scale. In this work, we consider in detail the possibility that SO(10) unification may also provide a natural dark matter candidate, stability being guaranteed by a leftover $\mathbb{Z}_2$ symmetry. We systematically examine the possible intermediate gauge groups which allow a nondegenerate, fermionic, Standard Model singlet dark matter candidate while at the same time respecting gauge coupling unification. Our analysis is done at the two-loop level. Surprisingly, despite the richness of SO(10), we find that only two models survive the analysis of phenomenological constraints, which include suitable neutrino masses, proton decay, and reheating.

DOI: 10.1103/PhysRevD.91.095010 PACS numbers: 95.35.+d, 12.10.Dm, 12.60.-i

I. INTRODUCTION

One of the often quoted motivations for supersymmetry (SUSY) is its ability to improve the possibility for gauge coupling unification at the grand unified (GUT) scale, which is not possible in minimal SU(5) [1]. However, SO(10) has the built-in possibility for achieving gauge coupling unification through several potential intermediate-scale gauge groups [2–4]. Of course, low-energy SUSY has many other motivations, including the presence of a dark matter (DM) candidate [5] whose stability is insured if R-parity is conserved. However, under very generic conditions, non-SUSY SO(10) models also possess a remnant $\mathbb{Z}_2$ symmetry when an intermediate-scale U(1) symmetry is broken [6–11]. Thus, several modest extensions of minimal SO(10) may also allow for the possibility of DM.

In building a successful SO(10), we must also require that the GUT and intermediate mass scales be sufficiently large so as to ensure a proton lifetime and neutrino masses compatible with experiment. Unfortunately, these requirements are not realized for every choice of intermediate-scale gauge group. The addition of a new SO(10) multiplet containing a DM candidate will, however, affect the running of the gauge couplings and can improve the desired unification of the gauge couplings. For this reason, we suppose that the DM candidate is charged under the intermediate gauge symmetries. The cosmological production of DM could occur, for example, out of equilibrium from the thermal bath (NonEquilibrium Thermal DM (NETDM) [4]) in a manner reminiscent of freeze-in scenarios [12]. This mechanism works with a stable particle which has no interaction with the SM particles. Thus, we focus on singlet DM candidates. Further, as scalar DM would most assuredly couple to the Standard Model (SM) Higgs, we limit our attention here to fermionic DM.

SO(10) grand unification is, of course, a general moniker for many candidate theories of unification, as there are several possible intermediate gauge groups and several possible choices for representations R_1 of Higgs fields which break SO(10) to the intermediate gauge group, $G_{\rm int}$, and then again, several possible choices of representations R_2 for the Higgs fields which break $G_{\rm int}$ down to the SM. Furthermore, there are several possible choices for the representation which contains DM. Thus, it may seem that DM in SO(10) models is a rather robust and generic feature. However, if we insist on maintaining gauge coupling unification at a suitably high scale to guarantee proton stability, the number of models is dramatically reduced. In fact, by limiting the dimension of the representation containing DM to be no larger than a **210**, we find that only two models survive.

In this paper, we will systematically examine the possibility for fermionic NETDM in SO(10) models, though our conclusions are more general than the specific NETDM model. We will discuss the various possible intermediate gauge groups and Higgs representations which allow for gauge coupling unification, and we will demonstrate the effect of including two-loop running of the renormalization group equations (RGEs). The DM representation needs to be split so that only fermions with the appropriate gauge quantum numbers survive at low energy. This requires fine-tuning similar to the doublet-triplet separation problem in GUTs. We also systematically consider viable DM representation and their effect on the running of the gauge couplings. In all but two distinct models, the presence of DM spoils the desired unification of the gauge couplings.

In the following, we begin by discussing the origin of a discrete symmetry in a variety of models with different intermediate gauge groups and the possible representations for DM and the splitting of the DM multiplet. In Sec. III, we first demonstrate gauge coupling unification in these models (without DM) and show the effect of including the two-loop functions in the RGE running and one-loop threshold effects. We next consider the question of gauge coupling unification in the presence of a DM multiplet. In Sec. IV, we discuss the criteria which select only two possible models in a specific example of the NETDM scenario [4]. The phenomenological aspects of these models including neutrino masses, proton decay, and the production of DM through reheating after inflation will be discussed in Sec. V. We also consider the case where the DM field is a singlet under the intermediate gauge groups in Sec. VI. Our conclusions will be given in Sec. VII.

II. CANDIDATES

We assume that the SO(10) gauge group is spontaneously broken to an intermediate subgroup $G_{\rm int}$ at the GUT scale $M_{\rm GUT}$, and subsequently broken to the SM gauge group $G_{\rm SM}$ at an intermediate scale $M_{\rm int}$:

$$\mathrm{SO}(10) \longrightarrow G_{\rm int} \longrightarrow G_{\rm SM} \otimes \mathbb{Z}_N, \tag{1}$$

with $G_{\rm SM} \equiv \mathrm{SU}(3)_C \otimes \mathrm{SU}(2)_L \otimes \mathrm{U}(1)_Y$. The Higgs multiplets which break SO(10) and $G_{\rm int}$ are called R_1 and R_2, respectively. In addition, we require that there be a remnant discrete symmetry $\mathbb{Z}_N$ that is capable of rendering a SM singlet field to be stable and hence account for the DM in the Universe [10,11]. The mechanism for ensuring a remnant $\mathbb{Z}_N$ is discussed in detail in Sec. II A, and the possible intermediate gauge groups that accommodate the condition are summarized in Sec. II B.

If, moreover, the DM couplings are such that the candidate is not in thermal equilibrium at early times, as in the NETDM scenario, we obtain stringent constraints on the model structure. We will consider this subject in Sec. II C.

A. Discrete symmetry in SO(10)

SO(10) is a rank-five group and has an extra U(1) symmetry beyond $\mathrm{U}(1)_Y$ in the SM gauge group. The U(1) charge assignment for fields in an SO(10) multiplet is determined uniquely up to an overall factor. We define the normalization factor such that all of the fields ϕ_i in a given model have integer charges Q_i with a minimum nonzero value of $|Q_i|$ equal to $+1$. Now, let us suppose that a Higgs field ϕ_H has a nonzero charge Q_H. Then, if $Q_H = 0$ (mod N) with $N \geq 2$ an integer, the U(1) symmetry is broken to a $\mathbb{Z}_N$ symmetry after the Higgs field obtains a vacuum expectation value (VEV) [7–9]. One can easily show this by noting that both the Lagrangian and the VEV $\langle \phi_H \rangle$ are invariant under the following transformations:

$$\phi_i \to \exp\left(\frac{i2\pi Q_i}{N}\right)\phi_i,$$
$$\langle \phi_H \rangle \to \exp\left(\frac{i2\pi Q_H}{N}\right)\langle \phi_H \rangle = \langle \phi_H \rangle. \tag{2}$$

Thus, an SO(10) GUT may account for the stability of DM in terms of the remnant $\mathbb{Z}_N$ symmetry originating from the extra U(1) gauge symmetry.

The next task is to determine which type of irreducible representations for the Higgs field ϕ_H can be exploited to realize the discrete symmetry. To that end, we follow the discussion presented in Ref. [13]. The discussion is based on the Dynkin formalism of the Lie algebra [14].[1] Since the rank of SO(10) is five, we have five independent generators which can be diagonalized simultaneously. We denote them by H_i ($i = 1, \ldots, 5$). They form the Cartan subalgebra of SO(10). Each component of a multiplet is characterized by a set of eigenvalues of the generators, μ_i ($i = 1, \ldots, 5$), called weights. We also define the weight vector $\boldsymbol{\mu} \equiv (\mu_1, \ldots, \mu_5)$. The weights in the adjoint representation are called roots α_i, with $\alpha = (\alpha_1, \ldots, \alpha_5)$ the root vector. Among the root vectors, a set of five linearly independent vectors play an important role. They are called simple roots, $\boldsymbol{\alpha}_i$ ($i = 1, \ldots 5$), and expressed by the Dynkin diagrams. In what follows, we consider the weight and root vectors in the so-called Dynkin basis. In this particularly useful basis, a weight vector $\boldsymbol{\mu}$ is expressed in terms of a set of Dynkin labels given by

$$\tilde{\mu}_i = \frac{2\boldsymbol{\alpha}_i \cdot \boldsymbol{\mu}}{|\boldsymbol{\alpha}_i|^2}. \tag{3}$$

It turns out that the Dynkin labels are always integers. For example, the highest weight of the **16** in SO(10) is expressed as $(0 \quad 0 \quad 0 \quad 0 \quad 1)$, while that of the **10** is given by $(1 \quad 0 \quad 0 \quad 0 \quad 0)$.

On the other hand, it is convenient to express the Cartan generators H_i in the dual basis, where they are expressed in terms of five-dimensional vectors $[\bar{h}_{i1}, \ldots, \bar{h}_{i5}]$ such that

[1] For a review and references, see Refs. [15,16]. We follow the convention of Ref. [15] in this paper.

their eigenvalues for a state corresponding to the weight $\boldsymbol{\mu}$ are given by

$$H_i(\boldsymbol{\mu}) = \sum_{j=1}^{5} \bar{h}_{ij}\tilde{\mu}_j. \tag{4}$$

We choose the five linearly independent Cartan generators as follows:

$$\begin{aligned}
H_1 &= \frac{1}{2}[1 \quad 2 \quad 2 \quad 1 \quad 1],\\
H_2 &= \frac{1}{2\sqrt{3}}[1 \quad 0 \quad 0 \quad -1 \quad 1],\\
H_3 &= \frac{1}{2}[0 \quad 0 \quad 1 \quad 1 \quad 1],\\
H_4 &= \frac{1}{6}[-2 \quad 0 \quad 3 \quad -1 \quad 1],\\
H_5 &= [2 \quad 0 \quad 2 \quad 1 \quad -1].
\end{aligned} \tag{5}$$

Here, H_1 and H_2 correspond to the $\mathrm{SU}(3)_C$ Cartan generators $\lambda_3/2$ and $\lambda_8/2$, respectively, where λ_A $(A = 1, \ldots, 8)$ are the Gell-Mann matrices; H_3 and H_4 are the weak isospin and hypercharge, T_{3L} and Y, respectively.[2] H_5 is related to the $B - L$ charge as $H_5 = -5(B - L) + 4Y$. The additional U(1) symmetry required to generate a discrete symmetry is provided by a linear combination of the Cartan generators containing H_5. Following Ref. [13] (see also Ref. [8]), we define the extra U(1) charge Q_1 by

$$Q_1 = -\frac{6}{5}H_4 - \frac{1}{5}H_5 = [0 \quad 0 \quad -1 \quad 0 \quad 0]. \tag{6}$$

This U(1) charge can be also written as $Q_1 = (B - L) - 2Y$. One can readily find that all of the components in **10** and **16** have the U(1) charges of either 0 or ± 1.

Now we consider possible representations, R_2, for ϕ_H discussed above. First, let us determine the possible weight vectors corresponding to the component of ϕ_H that can have a VEV without breaking the SM gauge group. Namely, such a component has a zero eigenvalue for H_i $(i = 1, \ldots, 4)$. This condition tells us that the corresponding weight vectors have the following form:

$$\boldsymbol{\mu}_N = (-N \quad N \quad -N \quad 0 \quad N). \tag{7}$$

The Q_1 charges of the vectors are then given by

$$Q_1(\boldsymbol{\mu}_N) = N. \tag{8}$$

It is found that the smallest irreducible representation that contains the weight vector $\boldsymbol{\mu}_N$ has the highest weight[3]

$$\Lambda_N = (0 \quad 0 \quad 0 \quad 0 \quad N). \tag{9}$$

Its dimension is $\mathbf{16}, \mathbf{126}, \mathbf{672}, \ldots$ for $N = 1, 2, 3, \ldots$, respectively.[4] To obtain a $\mathbb{Z}_N$ symmetry, $N \geq 2$ is required. Thus, as long as we consider relatively small representations (such as those with dimensions not exceeding 210), **126** is the only candidate[5] for the representation of ϕ_H. In this case, the remnant discrete symmetry is $\mathbb{Z}_2$.[6]

Under the $\mathbb{Z}_2$ symmetry, the SM left-handed fermions are even, while the SM right-handed fermions as well as the Higgs field are odd. One can easily show that this symmetry is related to the product of matter parity $P_M = (-1)^{3(B-L)}$ [19] and the $\mathrm{U}(1)_Y$ rotation by 6π, $e^{6i\pi Y}$. Thus, if a SM-singlet fermion (boson) has an even (odd) parity, the remnant $\mathbb{Z}_2$ symmetry makes the particle stable. In Table I, we summarize irreducible representations that contain $\boldsymbol{\mu}_N$. We only show those that have dimensions less than or equal to 210. From the table, we find that a singlet fermion in a **45**, **54**, **126**, or **210** representation, or a singlet scalar boson in a **16** or **144** representation, can be a DM candidate.

Note that although we need a **126** Higgs field to break the extra U(1) symmetry and produce a remnant $\mathbb{Z}_2$ symmetry, other $\mathbb{Z}_2$-even singlet fields, **45**, **54**, **210**, etc., can have VEVs simultaneously without breaking the $\mathbb{Z}_2$ symmetry. While the latter do not break the $\mathbb{Z}_2$ symmetry, as discussed above, they are not capable of producing it, thus requiring the **126**. We will use such fields to obtain an adequate mass spectrum and a nondegenerate DM candidate, as discussed in Sec. II C and Sec. IV. R_2 will therefore refer to all representations at the intermediate scale which are responsible for either symmetry breaking or intermediate-scale masses and may be a combination of the **126** and other representations listed in Table I with positive $\mathbb{Z}_2$ charge.

B. Intermediate gauge group

As shown in Eq. (1), the extra U(1) symmetry is assumed to be broken at the intermediate scale, i.e., the **126** Higgs

[2] In the case of the flipped SU(5) scenario [17,18], the weak hypercharge is given by $Y = -\frac{1}{5}(H_4 + H_5)$.

[3] In fact, we obtain $\boldsymbol{\mu}_N$ by subtracting the root vector $(1 \quad -1 \quad 1 \quad 0 \quad 0)$ from Λ_N N times.

[4] The dimension of Λ_N for any N is given by

$$\dim(\Lambda_N) = (1+N)\left(1+\frac{N}{2}\right)\left(1+\frac{N}{3}\right)^2\left(1+\frac{N}{4}\right)^2\left(1+\frac{N}{5}\right)^2 \times \left(1+\frac{N}{6}\right)\left(1+\frac{N}{7}\right). \tag{10}$$

[5] The next-to-smallest representation including $\boldsymbol{\mu}_2$ is **1728** with the highest weight $(1 \quad 0 \quad 0 \quad 1 \quad 1)$.

[6] For earlier work on the remnant $\mathbb{Z}_2$ symmetry in SO(10), see Ref. [6].

TABLE I. Irreducible representations containing $\boldsymbol{\mu}_N$.

	Representation	Highest weight	$\mathbb{Z}_2$
$\boldsymbol{\mu}_0$	**45**	(0 1 0 0 0)	+
	54	(2 0 0 0 0)	+
	210	(0 0 0 1 1)	+
$\boldsymbol{\mu}_1$	**16**	(0 0 0 0 1)	−
	144	(1 0 0 1 0)	−
$\boldsymbol{\mu}_2$	**126**	(0 0 0 0 2)	+

field acquires a VEV of the order of $M_{\rm int}$. Thus, the intermediate gauge group $G_{\rm int}$ should be of rank five. In Table II, we summarize the rank-five subgroups of SO(10) and the Higgs multiplets R_1 whose VEVs break SO(10) into the subgroups. Again, we only consider the representations whose dimensions are less than or equal to **210**. Here D denotes the so-called D-parity [20], that is, a $\mathbb{Z}_2$ symmetry with respect to the exchange of $SU(2)_L \leftrightarrow SU(2)_R$. D-parity can be related to an element of SO(10) [20] under which a fermion field transforms into its charge conjugate. In cases where the D-parity is not broken by R_1, it is subsequently broken by R_2 at the scale of $M_{\rm int}$. In the NETDM scenario, the reheating temperature is always below $M_{\rm int}$, and therefore any cosmological relics [6] due to the breaking of D-parity will be harmless. Note that the VEVs of the R_1 Higgs fields are even under the $\mathbb{Z}_2$ symmetry considered in Sec. II A. Thus, there is no danger for this $\mathbb{Z}_2$ symmetry to be spontaneously broken by the R_1 Higgs fields.

C. Fermion dark matter and degeneracy problem

In the NETDM scenario, the DM should not be in thermal equilibrium. This requirement disfavors scalar DM candidates, since a scalar, ϕ, can always have a quartic coupling with the SM Higgs field H: $\lambda_{\phi H}|\phi|^2|H|^2$. Unless $|\lambda_{\phi H}|$ is extremely small for some reason, this coupling keeps scalar DM in thermal equilibrium even when the temperature of the Universe becomes much lower than the reheating temperature. Therefore, we focus on fermionic DM in this paper. Following the discussion in Sec. II A, the DM candidate should be contained in either a **45**, **54**, **126**, or **210** representation.

TABLE II. Candidates for the intermediate gauge group $G_{\rm int}$.

$G_{\rm int}$	R_1
$SU(4)_C \otimes SU(2)_L \otimes SU(2)_R$	**210**
$SU(4)_C \otimes SU(2)_L \otimes SU(2)_R \otimes D$	**54**
$SU(4)_C \otimes SU(2)_L \otimes U(1)_R$	**45**
$SU(3)_C \otimes SU(2)_L \otimes SU(2)_R \otimes U(1)_{B-L}$	**45**
$SU(3)_C \otimes SU(2)_L \otimes SU(2)_R \otimes U(1)_{B-L} \otimes D$	**210**
$SU(3)_C \otimes SU(2)_L \otimes U(1)_R \otimes U(1)_{B-L}$	**45**, **210**
$SU(5) \otimes U(1)$	**45**, **210**
Flipped $SU(5) \otimes U(1)$	**45**, **210**

Below the GUT scale, components in an SO(10) multiplet can obtain different masses. We assume that only a part of an SO(10) multiplet which contains the DM candidate and forms a representation under $G_{\rm int}$ has a mass much lighter than the GUT scale. We denote this representation by $R_{\rm DM}$. Such a mass splitting can be realized by the Yukawa coupling of the DM multiplet with the R_1 Higgs field. After the R_1 Higgs obtains a VEV, the Yukawa coupling leads to an additional mass term for the SO(10) multiplet, which gives different masses among the components. By carefully choosing the parameters in the Lagrangian, we can make only $R_{\rm DM}$ light. This will be discussed in detail in Sec. IV.

As will be seen in Sec. III A, without $R_{\rm DM}$, SO(10) GUTs often predict a low value of either $M_{\rm GUT}$ or $M_{\rm int}$, which could be problematic for proton decay or the explanation of light neutrino masses, respectively. In order to affect the RGE running of the gauge couplings and possibly increase the mass scales for both $M_{\rm int}$ and $M_{\rm GUT}$, the DM should be charged under $G_{\rm int}$. In Table III, we summarize possible candidates for $R_{\rm DM}$ for each intermediate gauge group. Above the intermediate scale, all of the components have an identical mass. In fact, it turns out that the degeneracy is not resolved at tree level even after the intermediate gauge symmetry is broken. This is because the SO(10) multiplets which contain $R_{\rm DM}$ displayed in the table cannot have Yukawa couplings with the **126** Higgs; such a coupling is forbidden by the SO(10) symmetry. Thus, the effects of symmetry breaking by the **126** Higgs VEV cannot be transmitted to the mass of the $R_{\rm DM}$ multiplet at tree level, and a simple realization of DM in $R_{\rm DM}$ makes its components degenerate in mass.

Such a degenerate mass spectrum is problematic. Since the degenerate multiplet contains particles charged under the $SU(3)_C \otimes U(1)_{\rm EM}$ gauge group, they will be in thermal equilibrium. In general, these components have quite a long

TABLE III. Candidates for the NETDM.

$G_{\rm int}$	$R_{\rm DM}$	SO(10)
$SU(4)_C \otimes SU(2)_L \otimes SU(2)_R$	$(\mathbf{1},\mathbf{1},\mathbf{3})$	**45**
	$(\mathbf{15},\mathbf{1},\mathbf{1})$	**45**,**210**
	$(\mathbf{10},\mathbf{1},\mathbf{3})$	**126**
	$(\mathbf{15},\mathbf{1},\mathbf{3})$	**210**
$SU(4)_C \otimes SU(2)_L \otimes U(1)_R$	$(\mathbf{15},\mathbf{1},0)$	**45**,**210**
	$(\mathbf{10},\mathbf{1},1)$	**126**
$SU(3)_C \otimes SU(2)_L \otimes SU(2)_R \otimes U(1)_{B-L}$	$(\mathbf{1},\mathbf{1},\mathbf{3},0)$	**45**,**210**
	$(\mathbf{1},\mathbf{1},\mathbf{3},-2)$	**126**
$SU(3)_C \otimes SU(2)_L \otimes U(1)_R \otimes U(1)_{B-L}$	$(\mathbf{1},\mathbf{1},1,-2)$	**126**
$SU(5) \otimes U(1)$	$(\mathbf{24},0)$	**45**,**54**,**210**
	$(\mathbf{1},-10)$	**126**
	$(\mathbf{75},0)$	**210**
Flipped $SU(5) \otimes U(1)$	$(\mathbf{24},0)$	**45**,**54**,**210**
	$(\overline{\mathbf{50}},-2)$	**126**
	$(\mathbf{75},0)$	**210**

lifetime, and thus their thermal relic density conflicts with various observations. To see this, let us consider the $(\mathbf{1},\mathbf{1},\mathbf{3})$ Dirac fermion multiplet $(\psi^0,\psi^\pm)$ in the $\mathrm{SU}(4)_C\otimes\mathrm{SU}(2)_L\otimes\mathrm{SU}(2)_R$ theory, which originates from the **45** representation of SO(10), as an example. As mentioned above, they have an identical mass M at tree level, and the mass difference ΔM induced by the radiative corrections can be estimated as

$$\Delta M \simeq \frac{\alpha_1}{4\pi} M \ln\left(\frac{M_{\rm int}}{M}\right) \sim 0.01\times M, \qquad (11)$$

where α_1 is the U(1) gauge fine-structure constant. The charged components $\psi^\pm$ can decay into the neutral DM ψ^0 only through the exchange of the intermediate-scale gauge bosons as shown in Fig. 1. We estimate the decay width as

$$\Gamma(\psi^+\to\psi^0 f\bar{f}')\sim \frac{\alpha_R^2}{\pi}\frac{(\Delta M)^5}{M_{W_R}^4}, \qquad (12)$$

where $\alpha_R = g_R^2/4\pi$, and g_R and M_{W_R} are the coupling and the mass of the intermediate gauge boson W_R, respectively. Then, for example, when the DM mass is $\mathcal{O}(1)$ TeV and the intermediate scale is $\mathcal{O}(10^{13})$ GeV, the lifetime of ψ^+ is much longer than the age of the Universe, and thus cosmologically stable. The abundance of such a stable charged particle is stringently constrained by the null results of the search for heavy hydrogen in sea water [21]. The DM multiplets in other cases may also be accompanied by stable colored particles, whose abundance is severely restricted as well. If the intermediate scale is relatively low, the charged/colored particle can have a shorter lifetime. Even in this case, their thermal relic abundance should be extremely small in order not to spoil the success of big-bang nucleosynthesis (BBN). Quite generally, a degenerate mass spectrum leads to disastrous consequences. We refer to this problem as the "degeneracy problem" in what follows.

To avoid the degeneracy problem, we need to make the charged/colored components heavy enough so that they are not in thermal equilibrium and have very short lifetimes.

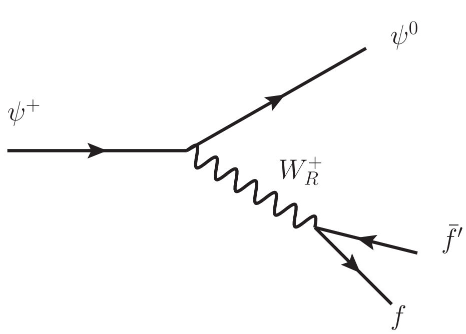

FIG. 1. Diagram responsible for the decay of ψ^+ into the DM ψ^0. f and f' denote the SM particles.

To that end, it is natural to explore a way to give them masses of $\mathcal{O}(M_{\rm int})$ by using the effects of the intermediate symmetry breaking. There are several solutions. One of the simplest ways is to introduce an additional Higgs field that has a VEV of the order of $M_{\rm int}$. For this purpose, we can use a **45**, **54**, or **210** field, as discussed in Sec. II A. The Yukawa coupling between the Higgs and the DM then yields the desired mass splitting. By fine-tuning the coupling, we can force only the DM to have a mass much below $M_{\rm int}$, while the other components remain around the intermediate scale.[7] Though other mechanisms are possible, we adopt this approach in this work. Concrete realizations of the mechanism are illustrated in Sec. IV.

Another solution to the degeneracy problem involves the use of higher-dimensional operators that include at least two **126** fields. One would expect that such operators suppressed by the Planck scale, $M_{\rm Pl}$, always exist. These Planck-suppressed operators can give rise to a mass difference of $\mathcal{O}(M_{\rm int}^2/M_{\rm Pl})$. Another mechanism to generate higher-dimensional operators is to introduce a vector-like fermion which has a Yukawa coupling with the DM and the **126** Higgs. By integrating out the fermion, we obtain dimension-five operators which give a $\mathcal{O}(M_{\rm int}^2/M_{\rm fer})$ mass difference, where $M_{\rm fer}$ is the mass of the additional fermion. Moreover, the higher-dimensional operators can be induced at the loop level, which gives rise to an $\mathcal{O}(\alpha_{\rm GUT}M_{\rm int}^2/(4\pi M_{\rm GUT}))$ mass difference, where $\alpha_{\rm GUT} = g_{\rm GUT}^2/(4\pi)$ is the fine-structure constant of the unified gauge coupling $g_{\rm GUT}$. Realization of these scenarios will be discussed elsewhere.

III. GAUGE COUPLING UNIFICATION

As is well known, gauge coupling unification can be realized in SO(10) GUTs with an intermediate scale [2].[8] Once the intermediate gauge group as well as the low-energy matter content is given, one can determine both the intermediate and GUT scales by requiring gauge coupling unification. In what follows, we reevaluate these scales in the SO(10) GUT scenarios with different intermediate gauge groups and up-to-date values for the input parameters. Then, in Sec. III B, we study the effects of the DM and the intermediate Higgs multiplets on gauge coupling unification. We will find that the requirement of gauge coupling unification severely constrains the NETDM models.

A. Gauge coupling unification with the intermediate scale

To begin with, let us briefly review SO(10) GUTs with an intermediate gauge group. In SO(10) GUTs, the SM

[7]This fine-tuning is similar to (though somewhat less severe than) the fine-tuning associated with the doublet-triplet separation to insure a weak scale Higgs boson.

[8]For a review, see Refs. [3,22].

fermions as well as three right-handed neutrinos are embedded into three copies of the **16** spinor representations, while the SM Higgs boson is usually included in a **10** representation. At the GUT scale, the SO(10) GUT group is spontaneously broken into an intermediate gauge group. Subsequently, the intermediate Higgs multiplet breaks it into the SM gauge group at the intermediate scale. In the following analysis, we work with the so-called extended survival hypothesis [23,24]; that is, we assume that a minimal set of Higgs multiplets necessary to realize the symmetry breaking exists in low-energy region. Above the intermediate scale, the presence of the additional Higgs multiplet and intermediate gauge bosons change the gauge coupling running from that in the SM. This makes it possible to realize gauge coupling unification in this scenario.

As displayed in Table II, the intermediate gauge groups relevant to our discussion are divided into two classes; those which contain the SU(5) group as a subgroup, and those which do not. The former class is, however, found to be less promising. In the case of ordinary $\mathrm{SU}(5)\otimes\mathrm{U}(1)$, the SM gauge couplings should meet at the intermediate scale, though they do not, as is well known. Failure of gauge coupling unification is also found in the flipped SU(5) case. This conclusion cannot be changed even if one adds the DM and Higgs multiplets in the case of ordinary SU(5). In the flipped SU(5) case, the addition of the DM and Higgs multiplets may yield gauge coupling unification. However, it turns out that the intermediate mass scale is as high as $\mathcal{O}(10^{17})$ GeV in such cases. Since the masses of the right-handed neutrinos are expected to be $\mathcal{O}(M_{\rm int})$, if $M_{\rm int}=\mathcal{O}(10^{17})$, the simple seesaw mechanism [25] cannot explain the neutrino masses required from the observation of the neutrino oscillations. However, the GUT scale tends to be close to the Planck scale, and one may need to rely on a double seesaw to explain neutrino masses [18,26]. We do not consider these possibilities in the following discussion.

The other class of the intermediate gauge groups is related to the Pati-Salam gauge group [27]. Therefore, it is useful to decompose the SO(10) multiplets into multiplets of the $\mathrm{SU}(4)_C\otimes\mathrm{SU}(2)_L\otimes\mathrm{SU}(2)_R$ gauge group. The **16** spinor representation in SO(10) is decomposed into a $(\mathbf{4},\mathbf{2},\mathbf{1})$ and $(\bar{\mathbf{4}},\mathbf{1},\mathbf{2})$ of $\mathrm{SU}(4)_C\otimes\mathrm{SU}(2)_L\otimes\mathrm{SU}(2)_R$. We denote them by Ψ_L and $\Psi_R^{\mathcal{C}}$, respectively, in which the SM fermions are embedded as follows:

$$\Psi_L=\begin{pmatrix} u_L^1 & u_L^2 & u_L^3 & \nu_L \\ d_L^1 & d_L^2 & d_L^3 & e_L \end{pmatrix},$$
$$\Psi_R^{\mathcal{C}}=\begin{pmatrix} d_{R1}^{\mathcal{C}} & d_{R2}^{\mathcal{C}} & d_{R3}^{\mathcal{C}} & e_R^{\mathcal{C}} \\ -u_{R1}^{\mathcal{C}} & -u_{R2}^{\mathcal{C}} & -u_{R3}^{\mathcal{C}} & -\nu_R^{\mathcal{C}} \end{pmatrix}, \tag{13}$$

where the indices represent the $\mathrm{SU}(3)_C$ color and $\mathcal{C}$ indicates charge conjugation. The SM Higgs field is, on the other hand, embedded in the $(\mathbf{1},\mathbf{2},\bar{\mathbf{2}})$ component of the ten-dimensional representation. As discussed in Ref. [28], to obtain the viable Yukawa sector,[9] we need to consider a complex scalar $\mathbf{10}_C$ for the representation, not a real one. Thus, $(\mathbf{1},\mathbf{2},\bar{\mathbf{2}})$ is also a complex scalar multiplet and includes the two Higgs doublets. In the following calculation, we regard one of these doublets as the SM Higgs boson, and the other is assumed to have a mass around the intermediate scale. The $\mathrm{SU}(4)_C\otimes\mathrm{SU}(2)_L\otimes\mathrm{SU}(2)_R$ gauge group is broken by the VEV of the $(\mathbf{10},\mathbf{1},\mathbf{3})$ component in the $\mathbf{126}_C$. In the presence of the left-right symmetry, we also have a $(\overline{\mathbf{10}},\mathbf{3},\mathbf{1})$ above the intermediate scale. We assume that the $(\overline{\mathbf{10}},\mathbf{3},\mathbf{1})$ field does not acquire a VEV, with which the constraint coming from the ρ parameter is avoided. From these charge assignments, one can readily obtain the quantum numbers for the corresponding fields in the other intermediate gauge groups, since they are subgroups of the $\mathrm{SU}(4)_C\otimes\mathrm{SU}(2)_L\otimes\mathrm{SU}(2)_R$.

With this field content, we study whether the gauge coupling unification is actually achieved or not for the first six intermediate gauge groups listed in Table II. We perform the analysis by using the two-loop RGEs, which are given in Appendix B. We will work in the $\overline{\mathrm{DR}}$ scheme [30], as there is no constant term in the intermediate and GUT scale matching conditions. The input parameters we use in our analysis are listed in Table VII in Appendix A. By solving the RGEs and assuming gauge coupling unification, we determine the intermediate scale $M_{\rm int}$, the GUT scale $M_{\rm GUT}$, and the unified gauge coupling constant $g_{\rm GUT}$. If we fail to find the appropriate values for these quantities, we will conclude that gauge coupling unification is not realized in this case. To determine their central values as well as the error coming from the input parameters, we form a χ^2 statistic as

$$\chi^2=\sum_{a=1}^{3}\frac{(g_a^2-g_{a,\rm exp}^2)^2}{\sigma^2(g_{a,\rm exp}^2)}, \tag{14}$$

where g_a are the gauge couplings at the electroweak scale obtained by solving the RGEs on the above assumption, and $g_{a,\rm exp}$ are the experimental values of the corresponding gauge couplings, with $\sigma(g_{a,\rm exp}^2)$ denoting their error. The central values of $M_{\rm int}$, $M_{\rm GUT}$, and $g_{\rm GUT}$ are corresponding to a point at which χ^2 is minimized.[10]

By using the method discussed above, we carry out the analysis and summarize the results in Table IV. Here, we show $\log_{10}(M_{\rm int})$, $\log_{10}(M_{\rm GUT})$, and $g_{\rm GUT}$. For each intermediate gauge group, the upper (lower) row shows the 2-loop (1-loop) result. $M_{\rm int}$ and $M_{\rm GUT}$ are given in GeV.

[9] For a general discussion on the Yukawa sector in SO(10) GUTs, see Refs. [28,29].

[10] We also use the χ^2 statistics to determine the value of the input Yukawa coupling in a similar manner, though it scarcely affects the error estimation of $M_{\rm int}$, $M_{\rm GUT}$, and $g_{\rm GUT}$.

The blank entries indicate that gauge coupling unification is not achieved. The uncertainties resulting from the input error are also shown in the parentheses. To illustrate our procedure more clearly, we show χ^2 as functions of $\log_{10}(M_{\rm int})$ (top), $\log(M_{\rm GUT})$ (middle), and $g_{\rm GUT}$ (bottom) in Fig. 2 for two examples of intermediate gauge groups. The left panels are for $G_{\rm int} = {\rm SU}(4)_C \otimes {\rm SU}(2)_L \otimes {\rm SU}(2)_R$, while the right ones are for $G_{\rm int} = {\rm SU}(4)_C \otimes {\rm SU}(2)_L \otimes {\rm SU}(2)_R \otimes D$. The χ^2 functions for the other choices of intermediate scale gauge groups will be qualitatively similar. Here again, $M_{\rm int}$ and $M_{\rm GUT}$ are given in GeV. In each plot, the other two free parameters are fixed to their best-fit values. We also plot the one-loop results (shown as dotted curves) to show the significance of the two-loop effects. In Fig. 3, we show the χ^2 functions projected down onto 2D planes corresponding to $g_{\rm GUT}$-$\log_{10}(M_{\rm int})$,

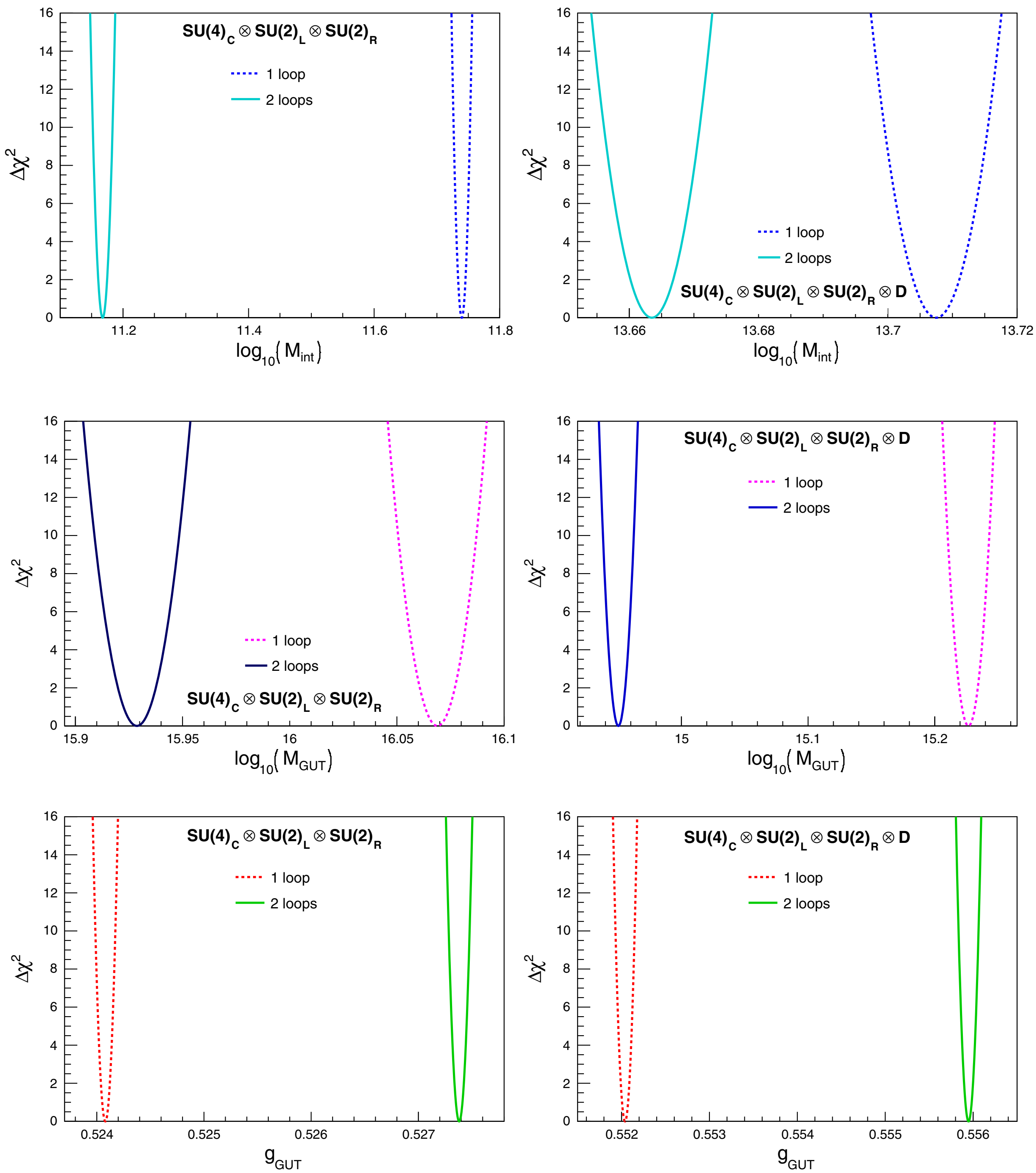

FIG. 2 (color online). χ^2 as functions of $\log_{10}(M_{\rm int})$ (top), $\log_{10}(M_{\rm GUT})$ (middle), and $g_{\rm GUT}$ (bottom). Left and right panels are for $G_{\rm int} = {\rm SU}(4)_C \otimes {\rm SU}(2)_L \otimes {\rm SU}(2)_R$ and $G_{\rm int} = {\rm SU}(4)_C \otimes {\rm SU}(2)_L \otimes {\rm SU}(2)_R \otimes D$, respectively. $M_{\rm int}$ and $M_{\rm GUT}$ are given in GeV.

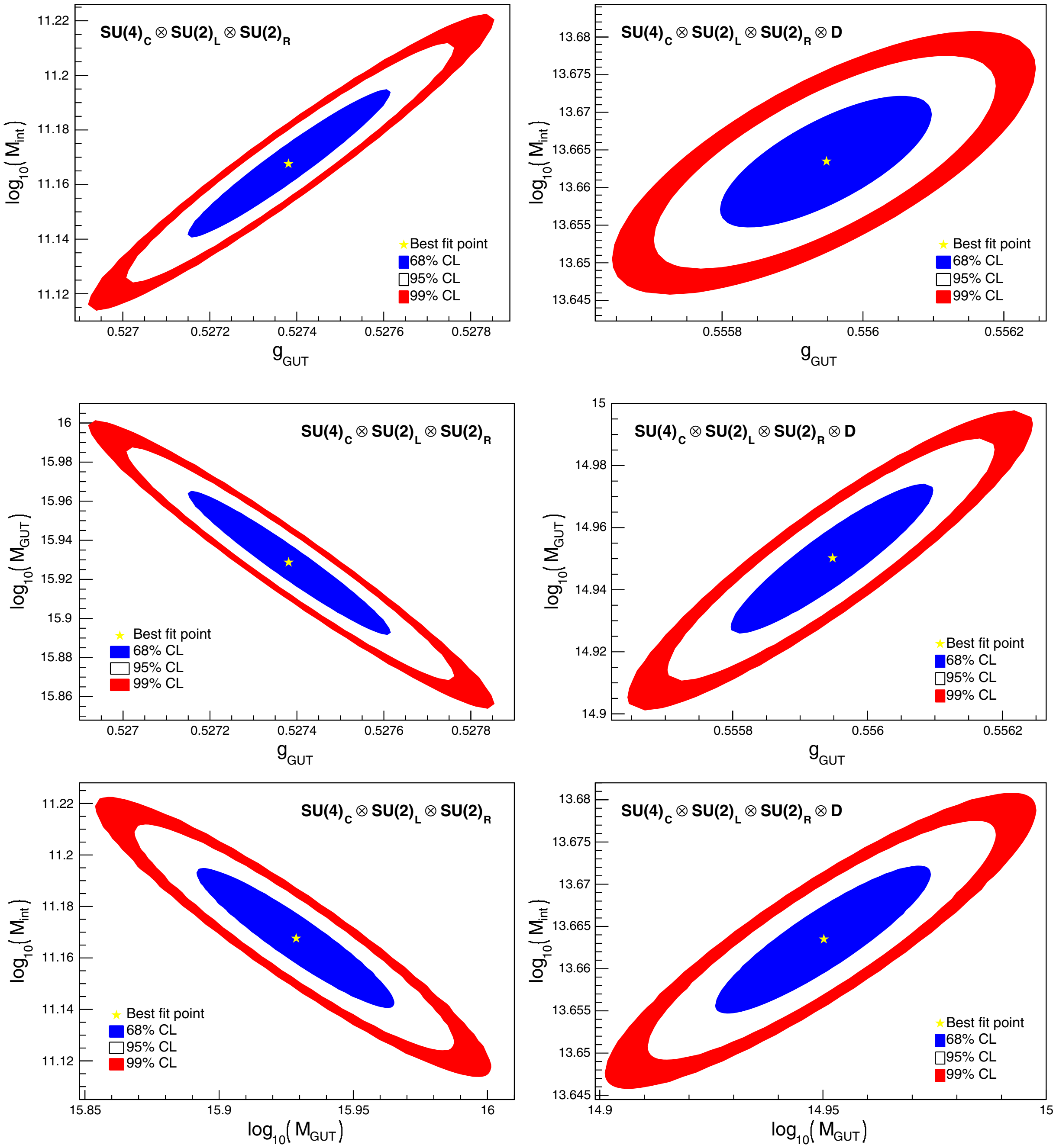

FIG. 3 (color online). Contour plots for the allowed region in the g_{GUT}-$\log_{10}(M_{\mathrm{int}})$, g_{GUT}-$\log_{10}(M_{\mathrm{GUT}})$, and $\log_{10}(M_{\mathrm{GUT}})$-$\log_{10}(M_{\mathrm{int}})$ parameter planes in the top, middle, and bottom panels, respectively. Left panels are for $G_{\mathrm{int}} = \mathrm{SU}(4)_C \otimes \mathrm{SU}(2)_L \otimes \mathrm{SU}(2)_R$, while right ones are for $G_{\mathrm{int}} = \mathrm{SU}(4)_C \otimes \mathrm{SU}(2)_L \otimes \mathrm{SU}(2)_R \otimes D$. Stars represent the best-fit point. The colored regions correspond to 68%, 95%, and 99% C.L. limits determined from $\Delta\chi^2 \simeq 2.30, 5.99, 9.21$.

g_{GUT}-$\log_{10}(M_{\mathrm{GUT}})$, and $\log_{10}(M_{\mathrm{GUT}})$-$\log_{10}(M_{\mathrm{int}})$ in the top, middle, and bottom panels, respectively. Again, the left panels are for $G_{\mathrm{int}} = \mathrm{SU}(4)_C \otimes \mathrm{SU}(2)_L \otimes \mathrm{SU}(2)_R$, while the ones on the right are for $G_{\mathrm{int}} = \mathrm{SU}(4)_C \otimes \mathrm{SU}(2)_L \otimes \mathrm{SU}(2)_R \otimes D$. The stars represent the best-fit point. The uncertainty ellipses represent 68%, 95%, and 99% C.L. uncertainties corresponding to $\Delta\chi^2 = 2.30$, 5.99, and 9.21, respectively. Threshold corrections at M_{int} and M_{GUT} [31] due to the nondegeneracy of the particles that have masses of the order of these scales contribute to the uncertainties.[11] For a recent discussion of threshold corrections, see Ref. [32]. In addition,

[11]Note that the intermediate scale in the left-right-symmetric theories does not depend on physics beyond M_{int}, as discussed in Appendix C.

TABLE IV. $\log_{10}(M_{\rm int})$, $\log_{10}(M_{\rm GUT})$, and $g_{\rm GUT}$. For each $G_{\rm int}$, the upper (lower) row shows the 2-loop (1-loop) result. $M_{\rm int}$ and $M_{\rm GUT}$ are given in GeV. The blank entries indicate that gauge coupling unification is not achieved.

$G_{\rm int}$	$\log_{10}(M_{\rm int})$	$\log_{10}(M_{\rm GUT})$	$g_{\rm GUT}$
$\mathrm{SU}(4)_C \otimes \mathrm{SU}(2)_L \otimes \mathrm{SU}(2)_R$	11.17(1)	15.929(4)	0.52738(4)
	11.740(8)	16.07(2)	0.5241(1)
$\mathrm{SU}(4)_C \otimes \mathrm{SU}(2)_L \otimes \mathrm{SU}(2)_R \otimes D$	13.664(3)	14.95(1)	0.5559(1)
	13.708(7)	15.23(3)	0.5520(1)
$\mathrm{SU}(4)_C \otimes \mathrm{SU}(2)_L \otimes \mathrm{U}(1)_R$	11.35(2)	14.42(1)	0.5359(1)
	11.23(1)	14.638(8)	0.53227(7)
$\mathrm{SU}(3)_C \otimes \mathrm{SU}(2)_L \otimes \mathrm{SU}(2)_R \otimes \mathrm{U}(1)_{B-L}$	9.46(2)	16.20(2)	0.52612(8)
	8.993(3)	16.68(4)	0.52124(3)
$\mathrm{SU}(3)_C \otimes \mathrm{SU}(2)_L \otimes \mathrm{SU}(2)_R \otimes \mathrm{U}(1)_{B-L} \otimes D$	10.51(1)	15.38(2)	0.53880(3)
	10.090(9)	15.77(1)	0.53478(6)
$\mathrm{SU}(3)_C \otimes \mathrm{SU}(2)_L \otimes \mathrm{U}(1)_R \otimes \mathrm{U}(1)_{B-L}$			

we neglect the contribution of Yukawa couplings above the intermediate scale, which causes additional error. These are expected to give $\mathcal{O}(1)\%$ uncertainty to the results.

From Table IV, it is found that gauge coupling unification is not achieved in the case of $G_{\rm int} = \mathrm{SU}(3)_C \otimes \mathrm{SU}(2)_L \otimes \mathrm{U}(1)_R \otimes \mathrm{U}(1)_{B-L}$. Moreover, we find that relatively low GUT scales are predicted for $G_{\rm int} = \mathrm{SU}(4)_C \otimes \mathrm{SU}(2)_L \otimes \mathrm{SU}(2)_R \otimes D$ and $\mathrm{SU}(4)_C \otimes \mathrm{SU}(2)_L \otimes \mathrm{U}(1)_R$, and thus the proton decay constraints may be severe in these cases, as discussed in Sec. V B. Furthermore, except for $G_{\rm int} = \mathrm{SU}(4)_C \otimes \mathrm{SU}(2)_L \otimes \mathrm{SU}(2)_R \otimes D$, we obtain low intermediate scales, with which it may be difficult to account for the neutrino masses, as explained in Sec. V A. As we will see below, this situation can be improved in the NETDM models.

B. NETDM and gauge coupling unification

Next, we look for the NETDM models in which gauge coupling unification is realized with an appropriate intermediate unification scale. Here, we require $10^{15} \lesssim M_{\rm GUT} \lesssim 10^{18}$ GeV; if $M_{\rm GUT} < 10^{15}$ GeV, then proton decays are too rapid to be consistent with proton decay experiments, while if $M_{\rm GUT} > 10^{18}$ GeV, then gravitational effects cannot be neglected anymore, and a calculation based on quantum field theories may be invalid around the GUT scale. To search for promising candidates, we assume the following conditions: First, a model should contain a NETDM candidate shown in Table III, where only a singlet component has a mass much below the intermediate scale. This component does not affect the running of the gauge couplings. Second, the rest of the components in $R_{\rm DM}$ are assumed to be around $M_{\rm int}$ due to the mass splitting mechanism with an additional Higgs multiplet, discussed in Sec. II C. At this point, we only assume that there exists an extra Higgs multiplet from either the **45**, **54** or **210** whose mass is around the intermediate scale. Whether the VEV of the extra Higgs actually gives rise to the mass splitting or not will be discussed in the subsequent section. Thirdly, we require that only the SM fields, the intermediate gauge bosons, $R_{\rm DM}$, and R_2 are present below the GUT scale. For

TABLE V. Models that realize the gauge coupling unification. $M_{\rm int}$ and $M_{\rm GUT}$ are given in GeV. All of the values listed here are evaluated at one-loop level.

$R_{\rm DM}$	R_2	$\log_{10}(M_{\rm int})$	$\log_{10}(M_{\rm GUT})$	$g_{\rm GUT}$
$\mathrm{SU}(4)_C \otimes \mathrm{SU}(2)_L \otimes \mathrm{SU}(2)_R$				
$(\mathbf{1},\mathbf{1},\mathbf{3})_W$	$(\mathbf{10},\mathbf{1},\mathbf{3})_C$ $(\mathbf{1},\mathbf{1},\mathbf{3})_R$	10.8	15.9	0.53
$(\mathbf{1},\mathbf{1},\mathbf{3})_D$	$(\mathbf{10},\mathbf{1},\mathbf{3})_C$ $(\mathbf{1},\mathbf{1},\mathbf{3})_R$	9.8	15.7	0.53
$\mathrm{SU}(4)_C \otimes \mathrm{SU}(2)_L \otimes \mathrm{SU}(2)_R \otimes D$				
$R_{\rm DM}$	R_2	$\log_{10}(M_{\rm int})$	$\log_{10}(M_{\rm GUT})$	$g_{\rm GUT}$
$(\mathbf{15},\mathbf{1},\mathbf{1})_W$	$(\mathbf{10},\mathbf{1},\mathbf{3})_C$ $(\overline{\mathbf{10}},\mathbf{3},\mathbf{1})_C$ $(\mathbf{15},\mathbf{1},\mathbf{1})_R$ $(\mathbf{10},\mathbf{1},\mathbf{3})_C$ $(\overline{\mathbf{10}},\mathbf{3},\mathbf{1})_C$	13.7	16.2	0.56
$(\mathbf{15},\mathbf{1},\mathbf{1})_W$	$(\mathbf{15},\mathbf{1},\mathbf{3})_R$ $(\mathbf{15},\mathbf{3},\mathbf{1})_R$ $(\mathbf{10},\mathbf{1},\mathbf{3})_C$ $(\overline{\mathbf{10}},\mathbf{3},\mathbf{1})_C$	14.2	15.5	0.56
$(\mathbf{15},\mathbf{1},\mathbf{1})_D$	$(\mathbf{15},\mathbf{1},\mathbf{3})_R$ $(\mathbf{15},\mathbf{3},\mathbf{1})_R$	14.4	16.3	0.58
$\mathrm{SU}(3)_C \otimes \mathrm{SU}(2)_L \otimes \mathrm{SU}(2)_R \otimes U(1)_{B-L}$				
$R_{\rm DM}$	R_2	$\log_{10}(M_{\rm int})$	$\log_{10}(M_{\rm GUT})$	$g_{\rm GUT}$
$(\mathbf{1},\mathbf{1},\mathbf{3},0)_W$	$(\mathbf{1},\mathbf{1},\mathbf{3},-2)_C$ $(\mathbf{1},\mathbf{1},\mathbf{3},0)_R$	6.1	16.6	0.52

example, if we consider the $(\mathbf{1},\mathbf{1},\mathbf{3})$ DM of the $\mathbf{45}$ given in the first column in Table III, then we suppose that all of the components of the $\mathbf{45}$ except $R_{\rm DM} = (\mathbf{1},\mathbf{1},\mathbf{3})$ should have masses around the GUT scale. This condition corresponds to the requirement of the minimal fine-tunings in the scalar potential to realize an adequate mass spectrum.

With these conditions, we then search for possible candidates by using the one-loop analytic formula given in Appendix C. In Table V, we summarize the field contents that satisfy the above requirements, as well as the values of $\log_{10}(M_{\rm int})$, $\log_{10}(M_{\rm GUT})$, and $g_{\rm GUT}$, with $M_{\rm int}$ and $M_{\rm GUT}$ in GeV. All of the values are evaluated at one-loop level. Here the subscript R, C, W, or D of each multiplet indicates that it is a real scalar, a complex scalar, a Weyl fermion, or a Dirac fermion, respectively. As for the intermediate Higgs fields, R_2, listed in Table V, $(\mathbf{10},\mathbf{1},\mathbf{3})_C$ and $(\mathbf{1},\mathbf{1},\mathbf{3},-2)_C$ are from the $\mathbf{126}$ Higgs field, while all other representations included in R_2 are extra Higgs fields introduced to resolve the degeneracy problem. For the additional Higgs fields, we only show the real scalar cases for brevity. Indeed, we can also consider complex scalars for the Higgs fields and find that gauge coupling unification is also realized in these cases, where both the intermediate and GUT scales are only slightly modified.

IV. MODELS

In the previous section, we have reduced the possible candidates to those presented in Table V. In this section, we study if any of those models are viable; i.e., we check if they actually offer appropriate an mass spectrum to realize the NETDM scenario, with the charged/colored components in $R_{\rm DM}$ acquiring masses of $\mathcal{O}(M_{\rm int})$.

First, let us consider the $(\mathbf{1},\mathbf{1},\mathbf{3})_{W/D}$ DM representation in the $\mathrm{SU}(4)_C \otimes \mathrm{SU}(2)_L \otimes \mathrm{SU}(2)_R$ gauge theory. To split the masses in the $(\mathbf{1},\mathbf{1},\mathbf{3})$ multiplet ψ^r, we need to couple the DM with the $(\mathbf{1},\mathbf{1},\mathbf{3})_R$ Higgs ϕ^r, with r denoting the $\mathrm{SU}(2)_R$ index. Since the fields transform as triplets under the $\mathrm{SU}(2)_R$ transformations, to construct an invariant term from the fields, the indices should be contracted antisymmetrically; i.e., the coupling should have a form like

$$\epsilon_{pqr}(\bar{\psi})^p\psi^q\phi^r. \tag{15}$$

Then, if ψ^r is a Majorana fermion, the above term always vanishes. Thus, ψ^r should be a Dirac fermion—that is, $(\mathbf{1},\mathbf{1},\mathbf{3})_D$ is the unique candidate for NETDM in this case.

Next, we study the terms in the SO(10) Lagrangian relevant to the masses of the fields much lighter than the GUT scale. In SO(10), $(\mathbf{1},\mathbf{1},\mathbf{3})_D$, $(\mathbf{1},\mathbf{1},\mathbf{3})_R$, and $(\mathbf{10},\mathbf{1},\mathbf{3})_C$ are included in the $\mathbf{45}_D$, $\mathbf{45}_R$, and $\mathbf{126}_C$, respectively. The SO(10) gauge group is spontaneously broken by the $\mathbf{210}_R$ Higgs field (R_1) into the $\mathrm{SU}(4)_C \otimes \mathrm{SU}(2)_L \otimes \mathrm{SU}(2)_R$ intermediate gauge group. As is usually done in the intermediate scale scenario, we fine-tune the Higgs potential so that the $(\mathbf{1},\mathbf{1},\mathbf{3})_R$ and $(\mathbf{10},\mathbf{1},\mathbf{3})_C$ Higgs fields have masses around the intermediate scale. This can always be performed by using the couplings of the $\mathbf{45}_R$ and $\mathbf{126}_C$ fields with the $\mathbf{210}_R$ Higgs field, which acquires a VEV of the order of the GUT scale. Similarly, we give desirable masses to the fields in $(\mathbf{1},\mathbf{1},\mathbf{3})_D$ by carefully choosing the couplings of the $\mathbf{45}_D$ fermion with the $\mathbf{45}_R$ and $\mathbf{126}_C$ Higgs fields. Here, the relevant interactions are

$$\mathcal{L}_{\rm int} = -M_{45_D}\overline{\mathbf{45}_D}\mathbf{45}_D - iy_{45}\overline{\mathbf{45}_D}\mathbf{45}_D\mathbf{45}_R - y_{210}\overline{\mathbf{45}_D}\mathbf{45}_D\mathbf{210}_R. \tag{16}$$

Notice that $\mathbf{45}_D$ does not couple to the $\mathbf{126}_C$ field, as already mentioned in Sec. II C. After the $R_1 = \mathbf{210}_R$ Higgs field gets a VEV $\langle\mathbf{210}_R\rangle = v_{210}$, the interactions in Eq. (16) lead to the following terms[12]:

$$\mathcal{L}_{\rm int} \to -M_{\rm DM}(\bar{\psi})^r\psi^r - iy_{45}\epsilon_{rst}(\bar{\psi})^r\psi^s\phi^t, \tag{17}$$

with $M_{\rm DM} = M_{45_D} + y_{210}v_{210}/\sqrt{6}$. Here, ψ^r and ϕ^r denote the $(\mathbf{1},\mathbf{1},\mathbf{3})_D$ and $(\mathbf{1},\mathbf{1},\mathbf{3})_R$ components in $\mathbf{45}_D$ and $\mathbf{45}_R$, respectively. We find that although M_{45_D} and v_{210} are expected to be $\mathcal{O}(M_{\rm GUT})$, we can let $M_{\rm DM}$ be much lighter than the GUT scale by carefully choosing the above parameters so that they cancel each other. In addition, it turns out that the mass term of the $(\mathbf{1},\mathbf{3},\mathbf{1})_D$ component in $\mathbf{45}_D$ is given by $M_{45_D} - y_{210}v_{210}/\sqrt{6}$. Thus, even if we fine-tune M_{45_D} and y_{210} to realize $M_{\rm DM} \ll M_{\rm GUT}$, the mass of $(\mathbf{1},\mathbf{3},\mathbf{1})_D$ is still around the GUT scale. This observation reflects the violation of the D-parity in this model. At this point, all of the components in ψ^r have identical masses (the "degeneracy problem"). Once the neutral component of ϕ^r acquires a VEV $\langle\phi^3\rangle = v_{45}$, which is assumed to be $\mathcal{O}(M_{\rm int})$, the second term in Eq. (17) gives rise to additional mass terms for ψ^r. These are

$$\mathcal{L}_{\rm int} \to -M_{\rm DM}\overline{\psi^0}\psi^0 - M_+\overline{\psi^+}\psi^+ - M_-\overline{\psi^-}\psi^-, \tag{18}$$

where $M_\pm = M_{\rm DM} \mp y_{45}v_{45}$, and ψ^0 and $\psi^\pm$ are the neutral and charged components, respectively.[13] The above expression shows that the VEV of the $\mathbf{45}_R$ Higgs field indeed solves the degeneracy problem; if $M_{\rm DM} \ll M_{\rm int}$ and $y_{45}v_{45} = \mathcal{O}(M_{\rm int})$, then the charged components acquire masses of $\mathcal{O}(M_{\rm int})$, while the neutral component has a mass much lighter than $M_{\rm int}$. Thus, we obtain the mass spectrum we have assumed in the previous section.

In the next example, we consider the DM representation $R_{\rm DM} = (\mathbf{15},\mathbf{1},\mathbf{1})_W$ with $R_2 = (\mathbf{10},\mathbf{1},\mathbf{3})_C \oplus (\overline{\mathbf{10}},\mathbf{3},\mathbf{1})_C \oplus (\mathbf{15},\mathbf{1},\mathbf{1})_R$ in the left-right-symmetric $\mathrm{SU}(4)_C \otimes \mathrm{SU}(2)_L \otimes \mathrm{SU}(2)_R$ gauge theory. In this case, $R_1 = \mathbf{54}_R$. We assume that the $(\mathbf{15},\mathbf{1},\mathbf{1})_W$ is a part of the $\mathbf{45}_W$, while

[12] For the computation of the Clebsch-Gordan coefficients, we have used the results given in Ref. [33].

[13] Note that since ψ^r are Dirac fermions, $(\psi^0)^{\mathcal{C}} \neq \psi^0$ and $(\psi^\pm)^{\mathcal{C}} \neq \psi^\mp$.

both $(\mathbf{10},\mathbf{1},\mathbf{3})_C$ and $(\overline{\mathbf{10}},\mathbf{3},\mathbf{1})_C$ are part of the $\mathbf{126}_C$. The couplings of the DM with the Higgs fields, as well as its mass term, are then given by

$$\mathcal{L}_{\rm int} = -\frac{M_{45_W}}{2}\mathbf{45}_W\mathbf{45}_W - \frac{y_{54}}{2}\mathbf{45}_W\mathbf{45}_W\mathbf{54}_R - \frac{y_{210}}{2}\mathbf{45}_W\mathbf{45}_W\mathbf{210}_R + \text{H.c.} \qquad (19)$$

Here, $(\mathbf{15},\mathbf{1},\mathbf{1})_R$ is included in the $\mathbf{210}_R$ field; we cannot use a $\mathbf{45}_R$ in this case, since the Weyl fermion $\mathbf{45}_W$ has no coupling to the $\mathbf{45}_R$.[14] As before, below the GUT scale, the VEV of $\mathbf{54}_R$, v_{54}, gives a common mass M to the $(\mathbf{15},\mathbf{1},\mathbf{1})_W$ multiplet with $M = M_{45_W} - y_{54}v_{54}/\sqrt{15}$. We can take $M = \mathcal{O}(M_{\rm int})$ by fine-tuning M_{45_W} and $y_{54}v_{54}$. The above Lagrangian then reduces to

$$\mathcal{L}_{\rm int} \to -\frac{M}{2}\psi^A\psi^A + \frac{2y_{210}}{\sqrt{3}}\text{Tr}(\psi\phi\psi) + \text{H.c.}, \qquad (20)$$

where ψ^A and ϕ^A denote the $(\mathbf{15},\mathbf{1},\mathbf{1})_W$ and $(\mathbf{15},\mathbf{1},\mathbf{1})_R$ fields, respectively, with $\psi \equiv \psi^A T^A$ and $\phi \equiv \phi^A T^A$; $A, B, C = 1, \ldots 15$ are the SU(4) adjoint indices, and T^A are the SU(4) generators. The mass degeneracy in this case is resolved by the VEV of the $\mathbf{210}_R$ field,

$$\langle\phi\rangle = \frac{v_{210}}{2\sqrt{6}}\text{diag}(1,1,1,-3), \qquad (21)$$

with which Eq. (20) leads to

$$\mathcal{L}_{\rm int} \to -\frac{M_{\rm DM}}{2}\psi^0\psi^0 - \frac{M_{\tilde{g}}}{2}\tilde{g}^A\tilde{g}^A - M_\xi\bar{\xi}_a\xi^a + \text{H.c.}, \qquad (22)$$

where ψ^0, $\tilde{g}^A$, ξ^a, and $\bar{\xi}_a$ are the color singlet, octet, triplet, and antitriplet components in $(\mathbf{15},\mathbf{1},\mathbf{1})_W$, respectively, with a denoting the color index, and

$$M_{\rm DM} = M + \frac{\sqrt{2}}{3}y_{210}v_{210}, \qquad (23)$$

$$M_{\tilde{g}} = M - \frac{1}{3\sqrt{2}}y_{210}v_{210}, \qquad (24)$$

$$M_\xi = M + \frac{1}{3\sqrt{2}}y_{210}v_{210}. \qquad (25)$$

Therefore, by carefully adjusting $y_{210}v_{210}$, we can make the DM ψ^0 much lighter than $M_{\rm int}$ while keeping the other components around the intermediate scale.

There are two more possible representations for $R_{\rm DM}$ for the left-right-symmetric $\text{SU}(4)_C \otimes \text{SU}(2)_L \otimes \text{SU}(2)_R$ intermediate gauge group given in Table V, namely $(\mathbf{15},\mathbf{1},\mathbf{1})_{W/D}$. In this case, however, one can readily conclude that the degeneracy problem cannot be solved by the $(\mathbf{15},\mathbf{1},\mathbf{3})_R$ and $(\mathbf{15},\mathbf{3},\mathbf{1})_R$ Higgs fields. This is because the Yukawa couplings between the DM and these Higgs fields are forbidden by the intermediate gauge symmetry. As a consequence, we can safely neglect these possibilities.

Finally, we discuss the model presented in the last column in Table V. We again find that the $(\mathbf{1},\mathbf{1},\mathbf{3},0)_R$ Higgs field does not yield a mass difference among the components in the $(\mathbf{1},\mathbf{1},\mathbf{3},0)_W$ DM multiplet, since the operator in Eq. (15) vanishes when the DM is a Weyl fermion. Thus, we do not consider this model in the following discussion.

As a result, we obtain two distinct models for NETDM within SO(10). We summarize these two models in Table VI. We call them models I and II in what follows. Here, $M_{\rm int}$ and $M_{\rm GUT}$ are given in GeV, and all of the values are evaluated with two-loop RGEs and differ somewhat from the one-loop values given in Table V. The errors shown in the parentheses arise from uncertainties in the input parameters. In addition, we again expect threshold corrections at $M_{\rm int}$ and $M_{\rm GUT}$. Furthermore, we neglect the contribution of Yukawa couplings to the RGEs above the intermediate scale, and this also will contribute to the theoretical error. We estimate that these two sources cause $\mathcal{O}(1)\%$ uncertainties in the values displayed in Table VI. From these results, we find that the presence of the DM component as well as the extra Higgs bosons can significantly alter the intermediate and GUT scales,[15] because of their effects on the gauge coupling running. To illustrate this more clearly, in Fig. 4 we show the running of gauge couplings in each theory. The left and right panels of Fig. 4 correspond to models I and II, respectively. In each figure, solid (dashed) lines show the case with (without) DM and additional Higgs bosons. The blue, green, and red lines represent the running of the U(1), SU(2) and SU(3) gauge couplings, respectively, where the U(1) fine-structure constant α_1 is defined by

$$\frac{1}{\alpha_1} \equiv \frac{3}{5}\frac{1}{\alpha_{2R}} + \frac{2}{5}\frac{1}{\alpha_4}, \qquad (26)$$

while the $\text{SU}(3)_C$ coupling α_3 is defined by $\alpha_3 \equiv \alpha_4$ above the intermediate scale. These figures clearly show the effects of the extra particles on the gauge coupling running. In particular, the GUT scale in model II is now well above 10^{15} GeV, which allows this model to evade the proton decay constraints, as will be seen in the subsequent section.

V. PHENOMENOLOGICAL ASPECTS

Now that we have obtained the NETDM models, we can study their phenomenological aspects and possible implications in future experiments. In Sec. V A, we first consider

[14] It is also possible to embed $(\mathbf{15},\mathbf{1},\mathbf{1})_W$ into $\mathbf{210}_W$ and $(\mathbf{15},\mathbf{1},\mathbf{1})_R$ into $\mathbf{45}_R$. The phenomenology in this case is the same as that discussed in the text.

[15] However, their existence hardly changes the intermediate scale in model II, which is clarified in Appendix C.

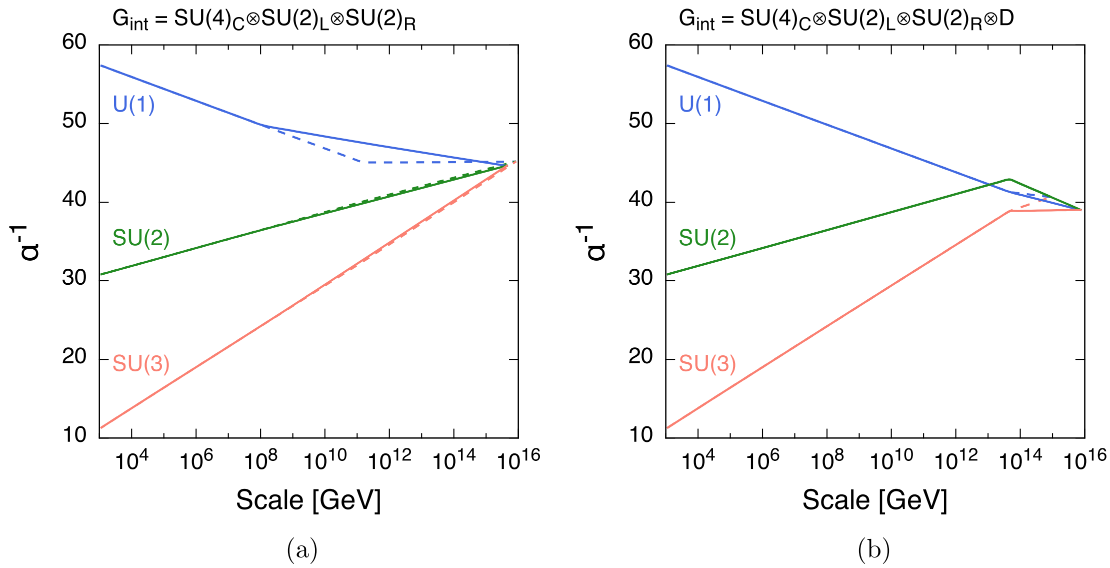

FIG. 4 (color online). Running of gauge couplings. Solid (dashed) lines show the case with (without) DM and additional Higgs bosons. Blue, green, and red lines represent the running of the U(1), SU(2) and SU(3) gauge couplings, respectively.

whether these models can give appropriate masses for light neutrinos. Next, in Sec. V B, we evaluate proton lifetimes in each model and discuss the testability in future proton decay experiments. Finally, we compute the abundance of DM produced by the NETDM mechanism in Sec. V C, and predict the reheating temperature after inflation.

A. Neutrino mass

In SO(10) GUTs, the Majorana mass terms of the right-handed neutrinos are induced after the $B-L$ symmetry is broken. These mass terms are generated from the Yukawa couplings of the **16** spinors with the $\mathbf{126}_C$ Higgs field. If the Yukawa couplings are $\mathcal{O}(1)$, then the Majorana mass terms are $\mathcal{O}(M_{\rm int})$. On the other hand, in these models, the Dirac masses of neutrinos are equal to the up-type quark masses, m_u, at the unification scale. Therefore, via the seesaw mechanism [25], light neutrino masses are given by

$$m_\nu \simeq \frac{m_u^2}{M_{\rm int}}. \qquad (27)$$

In model II, $M_{\rm int} = \mathcal{O}(10^{13})$ GeV indeed gives proper values for neutrino masses.[16] However, in model I, a low intermediate scale of $\mathcal{O}(10^8)$ GeV yields neutrino masses which are too heavy using the standard seesaw expression (27). Thus, model I is disfavored on the basis of small neutrino masses.

The defect in model I may be evaded if the $(\mathbf{15},\mathbf{2},\mathbf{2})$ component in $\mathbf{126}_C$ has a sizable mixing with the $(\mathbf{1},\mathbf{2},\bar{\mathbf{2}})$ Higgs boson and acquires a VEV of the order of the electroweak scale. In this case, the neutrino Yukawa couplings can differ from those of the up quark, and thus the relation (27) does not hold any more. For sizable mixing to occur, the $(\mathbf{15},\mathbf{2},\mathbf{2})$ field should lie around the intermediate scale. One might think that the presence of additional fields below the GUT scale would modify the running of the gauge couplings and spoil the above discussion based on gauge coupling unification. However, it turns out that both the intermediate and GUT scales are hardly affected by the existence of this field, though the unified gauge coupling constant becomes slightly larger. This is because its contribution to the one-loop beta function coefficients is $\Delta b_4 = 16/3$ and $\Delta b_{2L} = \Delta b_{2R} = 5$, and thus their difference is very tiny (see the discussion given in Appendix C). Therefore, we can take the $(\mathbf{15},\mathbf{2},\mathbf{2})$ to be at the intermediate scale with little change in the values of $M_{\rm int}$ and $M_{\rm GUT}$. The presence of the $(\mathbf{15},\mathbf{2},\mathbf{2})$ is also desirable to account for the down-type quark and charged lepton Yukawa couplings [28,35–37]. In addition, the higher-dimensional operators induced above the GUT scale may also affect the Yukawa couplings. Constructing a realistic Yukawa sector in these models is saved for future work.

B. Proton decay

Proton decay is a smoking-gun signature of GUTs, and thus a powerful tool for testing them. In non-SUSY GUTs,

[16]Note that in a left-right-symmetric model such as model II there is in general also a type-II seesaw contribution to m_ν from the VEV of the $SU(2)_L$ triplet in the $\mathbf{126}_C$. However, we know from constraints on the ρ parameter that the VEV must be quite small and definitely much smaller than the VEV of the $SU(2)_R$ triplet. For example, if the mixing between the $SU(2)_L$ and $SU(2)_R$ triplets with the Higgs doublets is small, it is safe to assume that the $SU(2)_L$ triplet VEV is small, and thus the type-II seesaw contribution is subdominant [34].

$p \to e^+\pi^0$ is the dominant decay mode, which is caused by the exchange of GUT-scale gauge bosons. This could be compared with the case of the SUSY GUTs; in SUSY GUTs, the color-triplet Higgs exchange usually yields the dominant contribution to proton decay, which gives rise to the $p \to K^+\bar{\nu}$ decay mode [38].[17]

Since the $p \to e^+\pi^0$ decay mode is induced by gauge interactions, we can make a robust prediction for the partial decay lifetime of this mode. Details of the calculation are given in Appendix D. By using the results given there, we evaluate the partial decay lifetime of the $p \to e^+\pi^0$ mode in each theory and plot it as a function of $M_X/M_{\rm GUT}$ (M_X denotes the mass of the GUT-scale gauge boson) in Fig. 5. Here, the blue and red solid lines represent models I and II, while the blue and red dashed lines represent the models without the DM and extra Higgs multiplets as given in Table IV, namely $G_{\rm int} = {\rm SU}(4)_C \otimes {\rm SU}(2)_L \otimes {\rm SU}(2)_R$ and $G_{\rm int} = {\rm SU}(4)_C \otimes {\rm SU}(2)_L \otimes {\rm SU}(2)_R \otimes D$, respectively. The shaded area shows the region which is excluded by the current experimental bound, $\tau(p \to e^+\pi^0) > 1.4 \times 10^{34}$ years [40,41]. We have varied the heavy gauge boson mass between $M_{\rm GUT}/2 \le M_X \le 2M_{\rm GUT}$, which reflects our ignorance of the GUT-scale mass spectrum. From this figure, we see that the existence of DM and Higgs multiplets produces a large effect on the proton decay lifetime. In particular, in the case of ${\rm SU}(4)_C \otimes {\rm SU}(2)_L \otimes {\rm SU}(2)_R \otimes D$, the predicted lifetime is so small that the present bound has already excluded the possibility. This conclusion can be evaded, however, once the DM and R_2 Higgs multiplets are included in the theory, as they raise the value of $M_{\rm GUT}$. Moreover, model I is now being constrained by the proton decay experiments. In this case, the inclusion of the DM and Higgs multiplets decreases $M_{\rm GUT}$. Future proton decay experiments, such as the Hyper-Kamiokande experiment [42], may offer much improved sensitivities (by about an order of magnitude), with which we can probe a wide range of parameter space in both models.

C. Nonequilibrium thermal dark matter

Finally, we evaluate the relic abundance of DM produced by the NETDM mechanism [4] in models I and II. In both of these models, the DM ψ^0 is produced in the early Universe via the exchange of the intermediate-scale particles. Therefore, the production rate is extremely small and their self-annihilation can be neglected. In addition, the produced DM cannot be in the thermal bath, since they have no renormalizable interactions with the SM particles. These two features characterize the NETDM mechanism; the DM is produced by SM particles in the thermal bath via the intermediate boson exchange, while they do not annihilate with each other nor attain thermal equilibrium.

[17]For recent analyses on proton decay in SUSY GUTs, see Ref. [39].

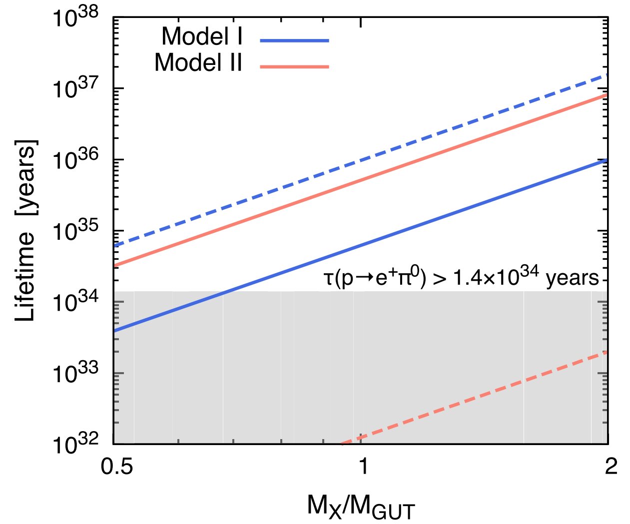

FIG. 5 (color online). Proton lifetimes as functions of $M_X/M_{\rm GUT}$. Blue solid and red solid lines represent model I and model II, respectively. Blue dashed and red dashed lines represent the cases for $G_{\rm int} = {\rm SU}(4)_C \otimes {\rm SU}(2)_L \otimes {\rm SU}(2)_R$ and $G_{\rm int} = {\rm SU}(4)_C \otimes {\rm SU}(2)_L \otimes {\rm SU}(2)_R \otimes D$ when the DM and extra Higgs multiplets are not included. The shaded area shows the region which is excluded by the current experimental bound, $\tau(p \to e^+\pi^0) > 1.4 \times 10^{34}$ years [40,41].

In what follows, we estimate the density of the DM produced via this mechanism and determine the reheating temperature which realizes the observed DM density.

The Boltzmann equation for the DM ψ^0 is given by

$$\frac{dY_{\rm DM}}{dx} = \sqrt{\frac{\pi}{45}} \frac{g_{*s}}{\sqrt{g_{*\rho}}} M_{\rm DM} M_{\rm Pl} \frac{\langle \sigma v \rangle}{x^2} Y_{\rm eq}^2, \tag{28}$$

with $Y_{\rm DM} \equiv n_{\rm DM}/s$ and $Y_{\rm eq} \equiv n_{\rm eq}/s$, where $n_{\rm DM}$ is the DM number density, $n_{\rm eq}$ is the equilibrium number density of each individual initial state SM particle, and s is the entropy of the Universe; $x \equiv M_{\rm DM}/T$, with T being the temperature of the Universe; g_{*s} and $g_{*\rho}$ are the effective degrees of freedom for the entropy and energy density in the thermal bath, respectively; $M_{\rm Pl} \equiv 1/\sqrt{G_N} = 1.22 \times 10^{19}$ GeV is the Planck mass; and $\langle \sigma v \rangle$ is the thermally averaged total annihilation cross section of the initial SM particles, f, into the DM pair. When we derive Eq. (28), we neglect the DM self-annihilation contribution as discussed above. From now on, we assume $g_{*s} = g_{*\rho} \equiv g_*$ for brevity.

We evaluate the thermal averaged cross section $\langle \sigma v \rangle$ multiplied by the equilibrium number density squared $n_{\rm eq}^2$ as

$$\langle \sigma v \rangle n_{\rm eq}^2 \simeq \frac{T}{512\pi^5} \int_{4M_{\rm DM}^2}^{\infty} d\hat{s} \sqrt{\hat{s} - 4M_{\rm DM}^2} K_1(\sqrt{\hat{s}}/T) \sum |\mathcal{M}|^2, \tag{29}$$

where $\sqrt{\hat{s}}$ denotes the center-of-mass energy, and $K_n(x)$ is the modified Bessel function of the second kind. Here, we

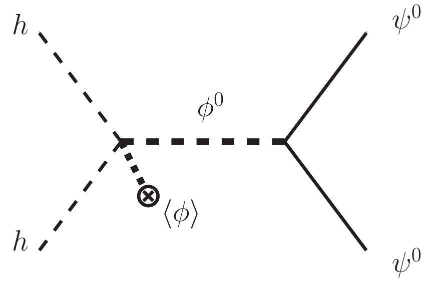

FIG. 6. Diagram responsible for the DM production in model II.

have used the approximation $m_f \ll \sqrt{\hat{s}}$, with m_f being the masses of the SM particles, since the particle production predominantly occurs at high temperature, and we have neglected the angular dependence of $\mathcal{M}$ for simplicity. In addition, we have assumed the initial particles follow a Maxwell-Boltzmann distribution and ignored statistical mechanical factors which may result from the Fermi-Dirac or Bose-Einstein distribution. $\sum|\mathcal{M}|^2$ indicates the sum of the squared amplitude over all possible incoming SM particles, as well as the spin of the final state.

Next, we evaluate the amplitude $\mathcal{M}$ in each model. First, we consider the case of model II. In this case, the dominant contribution comes from the tree-level Higgs-boson annihilation process displayed in Fig. 6. Here, ψ^0, h, and ϕ^0 denote the DM, the SM Higgs boson, and the singlet component of the $(\mathbf{15},\mathbf{1},\mathbf{1})_R$, respectively, and the VEV $\langle\phi\rangle$ is given in Eq. (21). From the dimensional analysis, we estimate the contribution as

$$\sum|\mathcal{M}|^2 \simeq c\,\frac{\hat{s}-4M_{\rm DM}^2}{M_{\rm int}^2}, \tag{30}$$

where c is a numerical factor which includes the unknown couplings appearing in the diagram. By substituting Eqs. (29) and (30) into Eq. (28), we have

$$\frac{dY_{\rm DM}}{dx} \simeq \frac{c}{1024\pi^7}\left(\frac{45}{\pi g_*}\right)^{\frac{3}{2}}\frac{M_{\rm Pl}M_{\rm DM}}{M_{\rm int}^2} \times \frac{1}{x^2}\int_{2x}^{\infty} t(t^2-4x^2)^{\frac{3}{2}}K_1(t)dt. \tag{31}$$

When $M_{\rm DM} \ll T_{\rm RH}$ with $T_{\rm RH}$ being the reheating temperature, the above equation is easily integrated to give

$$Y_{\rm DM}^{(0)} \simeq \frac{c}{64\pi^7}\left(\frac{45}{\pi g_*}\right)^{\frac{3}{2}}\frac{M_{\rm Pl}T_{\rm RH}}{M_{\rm int}^2}, \tag{32}$$

where the superscript "(0)" implies the present-day value. On the other hand, the current value of $Y_{\rm DM}^{(0)}$ is given by

$$Y_{\rm DM}^{(0)} = \frac{\Omega_{\rm DM}\rho_{\rm crit}^{(0)}}{M_{\rm DM}s^{(0)}}, \tag{33}$$

where $\Omega_{\rm DM}$ is the DM density parameter and $\rho_{\rm crit}^{(0)}$ is the critical density of the Universe. In the following calculation, we use $\Omega_{\rm DM}h^2 = 0.12$, $\rho_{\rm crit}^{(0)} = 1.05\times 10^{-5}h^2\ {\rm GeV}\cdot{\rm cm}^{-3}$, and $s^{(0)} = 2.89\times 10^3\ {\rm cm}^{-3}$, with h the Hubble parameter. As a result, we obtain

$$T_{\rm RH} \simeq 2.7\times 10^4\ {\rm GeV}\times\left(\frac{\Omega_{\rm DM}h^2}{0.12}\right)\left(\frac{g_*^{\frac{3}{2}}c^{-1}}{10^4}\right)\left(\frac{M_{\rm DM}}{100\ {\rm GeV}}\right)^{-1}, \tag{34}$$

where we have set the value of $M_{\rm int} = 10^{13.66}$ GeV from the result in Table VI. This approximate formula is valid when $M_{\rm DM} \ll T_{\rm RH}$. Here, $g_*^{\frac{3}{2}}c^{-1}$ is an unknown factor and thus causes an uncertainty in the computation. For instance, if $g_* = \mathcal{O}(100)$ and the quartic coupling of h and ϕ is ~ 0.3, then $g_*^{\frac{3}{2}}c^{-1} = \mathcal{O}(10^4)$. Note that the perturbativity of the quartic coupling ensures that this factor cannot become too small. On the other hand, it also has an upper bound; if c is extremely small, then the one-loop gauge-boson exchange contribution dominates over the tree level. Taking this consideration into account, we vary the value of $g_*^{\frac{3}{2}}c^{-1}$ by a factor of 10 to estimate the uncertainty in the analysis given below.

Next, we evaluate the relic abundance of the DM in model I. In this case, there is no tree-level process for the DM production, since the DM does not couple to the singlet component ϕ^0 in the $(\mathbf{1},\mathbf{1},\mathbf{3})_R$. Therefore, the DM is produced at the loop level. In Fig. 7, we show examples

TABLE VI. NETDM models. $M_{\rm int}$ and $M_{\rm GUT}$ are given in GeV. All of the values are evaluated with the two-loop RGEs.

	Model I	Model II
$G_{\rm int}$	$SU(4)_C\otimes SU(2)_L\otimes SU(2)_R$	$SU(4)_C\otimes SU(2)_L\otimes SU(2)_R\otimes D$
$R_{\rm DM}$	$(\mathbf{1},\mathbf{1},\mathbf{3})_D$ in $\mathbf{45}_D$	$(\mathbf{15},\mathbf{1},\mathbf{1})_W$ in $\mathbf{45}_W$
R_1	$\mathbf{210}_R$	$\mathbf{54}_R$
R_2	$(\mathbf{10},\mathbf{1},\mathbf{3})_C\oplus(\mathbf{1},\mathbf{1},\mathbf{3})_R$	$(\mathbf{10},\mathbf{1},\mathbf{3})_C\oplus(\mathbf{10},\mathbf{3},\mathbf{1})_C\oplus(\mathbf{15},\mathbf{1},\mathbf{1})_R$
$\log_{10}(M_{\rm int})$	8.08(1)	13.664(5)
$\log_{10}(M_{\rm GUT})$	15.645(7)	15.87(2)
$g_{\rm GUT}$	0.53055(3)	0.5675(2)

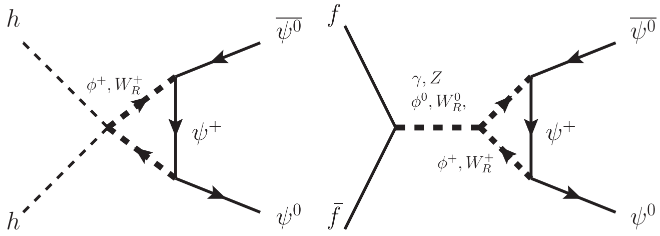

FIG. 7. Examples of diagrams responsible for the DM production in model I.

of one-loop diagrams which give the dominant contribution to the DM production. The amplitude is then estimated as

$$\sum |\mathcal{M}|^2 \simeq \frac{c'}{(16\pi^2)^2} \frac{\hat{s} - 4M_{\rm DM}^2}{M_{\rm int}^2}, \tag{35}$$

where we have included the one-loop factor. After a similar computation, we obtain

$$Y_{\rm DM}^{(0)} \simeq \frac{c'}{64\pi^7 (16\pi^2)^2} \left(\frac{45}{\pi g_*}\right)^{\frac{3}{2}} \frac{M_{\rm Pl} T_{\rm RH}}{M_{\rm int}^2} \tag{36}$$

and

$$T_{\rm RH} \simeq 4.6\ {\rm GeV} \times \left(\frac{\Omega_{\rm DM} h^2}{0.12}\right) \left(\frac{g_*^{\frac{3}{2}} c'^{-1}}{10^5}\right) \left(\frac{M_{\rm DM}}{\rm GeV}\right)^{-1} \tag{37}$$

on the assumption of $M_{\rm DM} \ll T_{\rm RH}$. Here, we have set $M_{\rm int} = 10^{8.08}$ GeV.

In Fig. 8, we plot the predicted reheating temperature as a function of the DM mass after numerically integrating Eq. (31). The left and right panels show the cases of models I and II, respectively. The pink band shows the uncertainty of the calculation, which we estimate by varying the unknown factor by a factor of 10. It turns out that when $M_{\rm DM} \ll T_{\rm RH}$, in the case of model I, only a small DM mass is allowed and the reheating temperature must be quite low. In model II, on the other hand, DM with a mass of around the electroweak scale accounts for the observed DM density with an acceptably high reheating temperature. For a larger $M_{\rm DM}$, in both models, the DM relic abundance can only be explained in the narrow strip region where $M_{\rm DM} \simeq T_{\rm RH}$.

VI. LONELY SINGLET FERMION DARK MATTER

In the above discussion, we have assumed that there exists a DM multiplet (as well as extra Higgs multiplets) above the intermediate scale, and studied how the presence of the additional fields affect the gauge coupling running in such models. As seen in Sec. III B, these fields can indeed improve the solutions for both the intermediate and GUT scales, which allow the models to evade the limit from the proton decay experiment and to explain light neutrino masses via the seesaw mechanism. Before concluding our discussion, we briefly consider another possibility in this section; that is, we have only a singlet DM fermion on top of the standard SO(10) setup discussed in Sec. III A. In this case, the DM, of course, cannot affect the gauge coupling running, and thus it does not solve the problems regarding the low intermediate/GUT scales in the ordinary SO(10) GUT models. Since there may be another solution to these problems, it is worthwhile studying this possibility as well.

In fact, we can easily construct such a model by exploiting an appropriate Higgs field at the GUT scale and fine-tuning its VEV so that only the singlet fermion

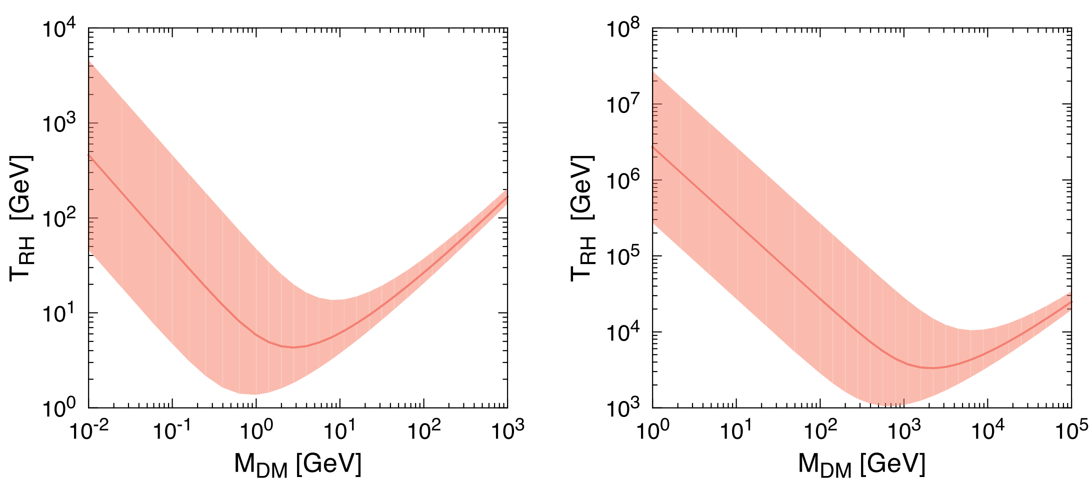

(a) (b)

FIG. 8 (color online). Reheating temperature as a function of DM mass. Pink band shows the theoretical uncertainty (a) Model I and (b) Model II.

DM has a mass much lighter than the GUT scale. For example, let us consider the case of $\mathrm{SU}(4)_C \otimes \mathrm{SU}(2)_L \otimes \mathrm{SU}(2)_R \otimes D$. In this case, the singlet field under the intermediate gauge interactions, $(\mathbf{1},\mathbf{1},\mathbf{1})$, is contained in a **54** or **210** of SO(10). Since only the **210** can have a Yukawa coupling to the $R_1 = \mathbf{54}_R$ Higgs field, we focus on the case where the singlet DM fermion is a component of the **210** field. In this case, both Majorana and Dirac fermions can couple to the R_1 Higgs. Then, by fine-tuning the Yukawa coupling, we can make only the singlet component have a light mass, as is done in Sec. IV. Similarly, we can obtain other models with different intermediate gauge groups by using appropriate multiplets for the fields which contain the singlet DM.

The NETDM mechanism again works for this singlet DM through the R_1 Higgs exchange process at tree level, with a diagram similar to that illustrated in Fig. 6. Following the discussion given in Sec. V C, we can readily evaluate the reheating temperature required to produce the right amount of DM. When $M_{\mathrm{DM}} \ll T_{\mathrm{RH}}$, we have

$$T_{\mathrm{RH}} \simeq 1.3 \times 10^9\ \mathrm{GeV} \times \left(\frac{\Omega_{\mathrm{DM}} h^2}{0.12}\right)\left(\frac{g_*^{\frac{3}{2}} c^{-1}}{10^4}\right) \times \left(\frac{M_{\mathrm{DM}}}{100\ \mathrm{GeV}}\right)^{-1}\left(\frac{M_{\mathrm{GUT}}}{10^{16}\ \mathrm{GeV}}\right)^2. \tag{38}$$

Compared with models I and II, the present scenario in general predicts a high reheating temperature, as the production occurs via the GUT-scale particle exchange. Such a high reheating temperature may be consistent with thermal leptogenesis [43].

As for proton decay and neutrino masses, the consequence of the singlet DM models is the same as that without DM. Thus, for $G_{\mathrm{int}} = \mathrm{SU}(4)_C \otimes \mathrm{SU}(2)_L \otimes \mathrm{SU}(2)_R \otimes D$ and $\mathrm{SU}(4)_C \otimes \mathrm{SU}(2)_L \otimes \mathrm{U}(1)_R$, the proton decay constraints are still problematic, and thus it may be required that we assume a relatively heavy GUT-scale gauge boson when compared to the GUT scale. Other intermediate groups are not suitable for the explanation of neutrino masses. The solution discussed in Sec. V A can again be exploited in these cases.

VII. CONCLUSION AND DISCUSSION

For over 40 years now, we have wondered whether grand unification is actually realized in nature. Its simplicity, its capacity for an explanation of charge quantization and the apparent focusing of the gauge couplings as they run to high energy has kept grand unification (supersymmetric or not) at the center of most ultraviolet completions of the SM, though experimental verification is still lacking.

On the other hand, we know from the existence of neutrino masses, the baryon asymmetry of the Universe, and the existence of DM that there must be new physics beyond the SM. The presence of a natural DM candidate in SUSY extensions of the SM (with conserved R-parity) is often taken to be one of the motivations for low-energy SUSY. The ingredients for the baryon asymmetry are contained in most grand unified theories (supersymmetric or not) including SU(5) and SO(10), and while a neutrino seesaw can be accomplished in SU(5) [by including the right-handed neutrino as a SU(5) singlet], it is more natural in SO(10).

We have, here, examined several breaking schemes of SO(10) which lead to gauge coupling unification (by altering the SM running of the gauge couplings at an intermediate scale), and contain a remnant $\mathbb{Z}_N$ symmetry which can account for the stability of DM. Having established the possible intermediate-scale gauge groups capable of both gauge coupling unification and of supporting a stable DM candidate, we considered specific possible representations (of dimension no larger than **210** for simplicity) which contain a suitable nondegenerate SM singlet DM candidate. If the DM candidate couples to the SM only through intermediate scale fields, it may never equilibrate in the early Universe after reheating, and its production from the thermal bath is an example of the NETDM scenario. Despite the fact that there are several possible intermediate-scale gauge groups to consider and many possible representations for the DM candidate and intermediate-scale Higgs fields needed to break the degeneracy in the DM multiplet, we found only two surviving models: one each based on $\mathrm{SU}(4)_C \otimes \mathrm{SU}(2)_L \otimes \mathrm{SU}(2)_R$ and $\mathrm{SU}(4)_C \otimes \mathrm{SU}(2)_L \otimes \mathrm{SU}(2)_R \otimes D$, with DM contained in a $(\mathbf{1},\mathbf{1},\mathbf{3})_D \in \mathbf{45}_D$ and $(\mathbf{15},\mathbf{1},\mathbf{1})_W \in \mathbf{45}_W$, respectively.

Both of the surviving models are capable of producing light neutrino masses (though it is more difficult in model I due to its relatively low intermediate scale). We also showed that while the proton decay lifetime (to $e^+\pi^0$) is at least a factor of 2 longer than the current experimental bound for $M_X/M_{\mathrm{GUT}} > 1/2$ in model I, the current bound excludes masses $M_X/M_{\mathrm{GUT}} \lesssim 0.7$, and higher masses may be probed in future proton decay experiments. Finally, within the NETDM production scenario, we have related our two models to a specific reheat temperature after inflation needed to obtain the current relic density. While model II predicts a reheat temperature which easily allows for (nonthermal) leptogenesis [43,44], the reheat temperature in model I is rather low and presents a challenge for baryogenesis.

ACKNOWLEDGMENTS

Florian Lyonnet is gratefully acknowledged for useful discussions. This work was supported by the Spanish MICINN's Consolider-Ingenio 2010 program under Grant Multi-Dark No. CSD2009-00064, and Contract No. FPA2010-17747. Y. M. is grateful to the Mainz Institute for Theoretical Physics (MITP) for its hospitality and its partial support during the completion of this work.

Y. M. acknowledges partial support from the European Union FP7 ITN INVISIBLES (Marie Curie Actions, No. PITN-GA-2011-289442) and the ERC advanced grants MassTeV and Higgs@LHC. The work of N. N. is supported by research fellowships of the Japan Society for the Promotion of Science for Young Scientists. The work of K. A. O. and J. Z. was supported in part by DOE Grant No. DE-SC0011842 at the University of Minnesota. The work of J. Q. was supported by STFC Grant No. ST/J002798/1.

APPENDIX A: INPUT PARAMETERS

The values for the input parameters we have used in this paper are summarized in Table VII. They are taken from Ref. [45] except for the top-quark pole mass and the Higgs mass, for which we use the values given in Refs. [46] and [47], respectively. In this table, the gauge coupling constants are defined in the $\overline{\rm MS}$ scheme, and thus we convert them to the $\overline{\rm DR}$ scheme at the electroweak scale using the one-loop relation [48]:

$$g_a(m_Z)_{\overline{\rm DR}} = g_a(m_Z)_{\overline{\rm MS}}\left(1+\frac{C(G_a)\alpha_a(m_Z)_{\overline{\rm MS}}}{24\pi}\right), \qquad (A1)$$

where $C(G_a)$ is the quadratic Casimir invariant. For the mass of the top quark, we convert the pole mass to its $\overline{\rm MS}$ mass by using [45]

$$m_t^{\overline{\rm MS}}(m_t^{\overline{\rm MS}}) = m_t\left(1-\frac{4\alpha_s(m_t^{\overline{\rm MS}})}{3\pi}\right), \qquad (A2)$$

from which we obtain the $\overline{\rm MS}$ top Yukawa coupling. The $\overline{\rm DR}$ Yukawa coupling is then given by

$$y_t^{\overline{\rm DR}} = y_t^{\overline{\rm MS}}\left[1+\frac{\alpha_1}{480\pi}+\frac{3\alpha_2}{32\pi}-\frac{\alpha_3}{3\pi}\right]. \qquad (A3)$$

TABLE VII. Input parameters [45–47].

Strong coupling constant	$\alpha_s(m_Z)$	0.1185(6)
QED coupling constant	$\alpha(m_Z)$	1/127.944(14)
Fermi coupling constant	G_F	$1.1663787(6)\times10^{-5}\,\mathrm{GeV}^{-2}$
Weak mixing angle	$\sin^2\theta_W(m_Z)$	0.23126(5)
Z-boson mass	m_Z	91.1876(21) GeV
Top pole mass	m_t	173.34(82) GeV
Higgs mass	m_h	125.15(24) GeV

APPENDIX B: RENORMALIZATION GROUP EQUATIONS

In this section, we summarize the RGEs and the matching conditions used in text. The two-loop RGEs [49] of the gauge coupling constants g_a are written as

$$\mu\frac{dg_a}{d\mu} = \frac{b_a^{(1)}}{16\pi^2}g_a^3 + \frac{g_a^3}{(16\pi^2)^2}\left[\sum_{b=1}^{3} b_{ab}^{(2)}g_b^2 - c_a y_t^2\right]. \qquad (B1)$$

Below, we will give the coefficients in each theory discussed in this paper. For the contribution of Yukawa couplings, we include them only in the SM running, as unknown Yukawa couplings appear above the intermediate scale. Their effects should be taken into account as theoretical uncertainties. All of the one-loop RGEs have been checked with the code PyR@TE [50], and more importantly, the two-loop RGEs have been computed with this code.

1. Standard Model

In the SM, we have

$$b_a^{(1)} = \begin{pmatrix} 41/10 \\ -19/6 \\ -7 \end{pmatrix},$$
$$b_{ab}^{(2)} = \begin{pmatrix} 199/50 & 27/10 & 44/5 \\ 9/10 & 35/6 & 12 \\ 11/10 & 9/2 & -26 \end{pmatrix},$$
$$c_a = \begin{pmatrix} 17/10 \\ 3/2 \\ 2 \end{pmatrix}. \qquad (B2)$$

Here, $a = 1, 2, 3$ correspond to U(1), $\mathrm{SU}(2)_L$, and $\mathrm{SU}(3)_C$, respectively, with the U(1) gauge coupling constant normalized as $g_1 \equiv \sqrt{5/3}g'$. Since the top Yukawa coupling contributes to the running of the gauge couplings at the two-loop level, it is sufficient to consider the one-loop RGE for the top Yukawa coupling. Furthermore, we can safely neglect the contribution of the other Yukawa couplings. Thus, the relevant RGE is

$$\mu\frac{d}{d\mu}y_t = \frac{1}{16\pi^2}y_t\left[\frac{9}{2}y_t^2 - \frac{17}{20}g_1^2 - \frac{9}{4}g_2^2 - 8g_3^2\right]. \qquad (B3)$$

2. $\mathbf{SU(4)_C \otimes SU(2)_L \otimes SU(2)_R}$

As discussed in Sec. III A, above the intermediate mass scale, the theory contains the SM fermions, the gauge bosons, the $(\mathbf{10},\mathbf{1},\mathbf{3})_C$ field, and the $(\mathbf{1},\mathbf{2},\bar{\mathbf{2}})_C$ Higgs field. The beta-function coefficients in this case are given by

$$b_a^{(1)} = \begin{pmatrix} -3 \\ 11/3 \\ -23/3 \end{pmatrix},$$
$$b_{ab}^{(2)} = \begin{pmatrix} 8 & 3 & 45/2 \\ 3 & 584/3 & 765/2 \\ 9/2 & 153/2 & 643/6 \end{pmatrix}, \quad \text{(B4)}$$

where $a = 2L, 2R, 4$ correspond to $\mathrm{SU}(2)_L$, $\mathrm{SU}(2)_R$, and $\mathrm{SU}(4)_C$, respectively. The matching conditions at the intermediate mass scale are

$$\frac{1}{g_1^2(M_{\rm int})} = \frac{3}{5}\frac{1}{g_{2R}^2(M_{\rm int})} + \frac{2}{5}\frac{1}{g_4^2(M_{\rm int})},$$
$$g_2(M_{\rm int}) = g_{2L}(M_{\rm int}),$$
$$g_3(M_{\rm int}) = g_4(M_{\rm int}). \quad \text{(B5)}$$

3. $\mathbf{SU(4)_C \otimes SU(2)_L \otimes SU(2)_R \otimes \mathit{D}}$

In this case, the $(\overline{\mathbf{10}}, \mathbf{3}, \mathbf{1})_C$ field is added to the previous theory. The beta-function coefficients then become

$$b_a^{(1)} = \begin{pmatrix} 11/3 \\ 11/3 \\ -14/3 \end{pmatrix},$$
$$b_{ab}^{(2)} = \begin{pmatrix} 584/3 & 3 & 765/2 \\ 3 & 584/3 & 765/2 \\ 153/2 & 153/2 & 1759/6 \end{pmatrix}, \quad \text{(B6)}$$

where $a = 2L, 2R, 4$ correspond to $\mathrm{SU}(2)_L$, $\mathrm{SU}(2)_R$, and $\mathrm{SU}(4)_C$, respectively.

4. $\mathbf{SU(4)_C \otimes SU(2)_L \otimes U(1)_R}$

This theory contains the SM fermions, the gauge bosons, the $(\mathbf{10}, \mathbf{1}, 1)_C$ field, and the $(\mathbf{1}, \mathbf{2}, \frac{1}{2})$ Higgs field. The beta-function coefficients in this case are given by

$$b_a^{(1)} = \begin{pmatrix} -19/6 \\ 15/2 \\ -29/3 \end{pmatrix},$$
$$b_{ab}^{(2)} = \begin{pmatrix} 35/6 & 1/2 & 45/2 \\ 3/2 & 87/2 & 405/2 \\ 9/2 & 27/2 & -101/6 \end{pmatrix}, \quad \text{(B7)}$$

where $a = 2L, 1R, 4$ correspond to $\mathrm{SU}(2)_L$, $U(1)_R$, and $\mathrm{SU}(4)_C$, respectively. The matching conditions at the intermediate mass scale are

$$\frac{1}{g_1^2(M_{\rm int})} = \frac{3}{5}\frac{1}{g_{1R}^2(M_{\rm int})} + \frac{2}{5}\frac{1}{g_4^2(M_{\rm int})},$$
$$g_2(M_{\rm int}) = g_{2L}(M_{\rm int}),$$
$$g_3(M_{\rm int}) = g_4(M_{\rm int}). \quad \text{(B8)}$$

5. $\mathbf{SU(3)_C \otimes SU(2)_L \otimes SU(2)_R \otimes U(1)_{\mathit{B-L}}}$

This theory contains the SM fermions, the gauge bosons, the $(\mathbf{1}, \mathbf{1}, \mathbf{3}, -2)_C$ field, and the $(\mathbf{1}, \mathbf{2}, \mathbf{2}, 0)$ Higgs field. The beta-function coefficients in this case are given by

$$b_a^{(1)} = \begin{pmatrix} -3 \\ -7/3 \\ 11/2 \\ -7 \end{pmatrix},$$
$$b_{ab}^{(2)} = \begin{pmatrix} 8 & 3 & 3/2 & 12 \\ 3 & 80/3 & 27/2 & 12 \\ 9/2 & 81/2 & 61/2 & 4 \\ 9/2 & 9/2 & 1/2 & -26 \end{pmatrix}, \quad \text{(B9)}$$

where $a = 2L, 2R, BL, 3$ correspond to $\mathrm{SU}(2)_L$, $\mathrm{SU}(2)_R$, $\mathrm{U}(1)_{B-L}$ and $\mathrm{SU}(3)_C$, respectively. The $\mathrm{U}(1)_{B-L}$ charge is normalized such that it satisfies the normalization condition of the SO(10) generators: $T_{B-L} = \sqrt{3/8}(B-L)$. The matching conditions at the intermediate mass scale are

$$\frac{1}{g_1^2(M_{\rm int})} = \frac{3}{5}\frac{1}{g_{2R}^2(M_{\rm int})} + \frac{2}{5}\frac{1}{g_{BL}^2(M_{\rm int})},$$
$$g_2(M_{\rm int}) = g_{2L}(M_{\rm int}),$$
$$g_3(M_{\rm int}) = g_3(M_{\rm int}). \quad \text{(B10)}$$

6. $\mathbf{SU(3)_C \otimes SU(2)_L \otimes SU(2)_R \otimes U(1)_{\mathit{B-L}} \otimes \mathit{D}}$

For this left-right-symmetric theory, the $(\mathbf{1}, \mathbf{3}, \mathbf{1}, 2)_C$ field is added to the previous case. The beta-function coefficients are then modified to

$$b_a^{(1)} = \begin{pmatrix} -7/3 \\ -7/3 \\ 7 \\ -7 \end{pmatrix},$$
$$b_{ab}^{(2)} = \begin{pmatrix} 80/3 & 3 & 27/2 & 12 \\ 3 & 80/3 & 27/2 & 12 \\ 81/2 & 81/2 & 115/2 & 4 \\ 9/2 & 9/2 & 1/2 & -26 \end{pmatrix}, \quad \text{(B11)}$$

where $a = 2L, 2R, BL, 3$ correspond to $\mathrm{SU}(2)_L$, $\mathrm{SU}(2)_R$, $\mathrm{U}(1)_{B-L}$ and $\mathrm{SU}(3)_C$, respectively.

7. $\mathbf{SU(3)_C \otimes SU(2)_L \otimes U(1)_R \otimes U(1)_{B-L}}$

This theory contains the SM fermions, the gauge bosons, the $(\mathbf{1},\mathbf{1},\mathbf{1},-2)_C$ field, and the $(\mathbf{1},\mathbf{2},1/2,0)$ Higgs field. The beta-function coefficients in this case are given by

$$b_a^{(1)} = \begin{pmatrix} -19/6 \\ 9/2 \\ 9/2 \\ -7 \end{pmatrix},$$
$$b_{ab}^{(2)} = \begin{pmatrix} 35/6 & 1/2 & 3/2 & 12 \\ 3/2 & 15/2 & 15/2 & 12 \\ 9/2 & 15/2 & 25/2 & 4 \\ 9/2 & 3/2 & 1/2 & -26 \end{pmatrix}, \tag{B12}$$

where $a = 2L, 1R, BL, 3$ correspond to $\mathrm{SU}(2)_L$, $U(1)_R$, $\mathrm{U}(1)_{B-L}$, and $\mathrm{SU}(3)_C$, respectively. The matching conditions at the intermediate mass scale are

$$\begin{aligned} \frac{1}{g_1^2(M_{\rm int})} &= \frac{3}{5}\frac{1}{g_{1R}^2(M_{\rm int})} + \frac{2}{5}\frac{1}{g_{BL}^2(M_{\rm int})}, \\ g_2(M_{\rm int}) &= g_{2L}(M_{\rm int}), \\ g_3(M_{\rm int}) &= g_3(M_{\rm int}). \end{aligned} \tag{B13}$$

8. Model I

For DM model I, a $(\mathbf{1},\mathbf{1},\mathbf{3})_D$ Dirac fermion and a $(\mathbf{1},\mathbf{1},\mathbf{3})_R$ real scalar field are added to the theory described in Appendix B 2. The beta-function coefficients are then computed as

$$b_a^{(1)} = \begin{pmatrix} -3 \\ 20/3 \\ -23/3 \end{pmatrix},$$
$$b_{ab}^{(2)} = \begin{pmatrix} 8 & 3 & 45/2 \\ 3 & 740/3 & 765/2 \\ 9/2 & 153/2 & 643/6 \end{pmatrix}, \tag{B14}$$

where $a = 2L, 2R, 4$ correspond to $\mathrm{SU}(2)_L$, $\mathrm{SU}(2)_R$, and $\mathrm{SU}(4)_C$, respectively.

9. Model II

For DM model II, a $(\mathbf{15},\mathbf{1},\mathbf{1})_W$ Weyl fermion and a $(\mathbf{15},\mathbf{1},\mathbf{1})_R$ real scalar field are added to the theory described in Appendix B 3. The beta-function coefficients are then computed as

$$b_a^{(1)} = \begin{pmatrix} 11/3 \\ 11/3 \\ -4/3 \end{pmatrix},$$
$$b_{ab}^{(2)} = \begin{pmatrix} 584/3 & 3 & 765/2 \\ 3 & 584/3 & 765/2 \\ 153/2 & 153/2 & 2495/6 \end{pmatrix}, \tag{B15}$$

where $a = 2L, 2R, 4$ correspond to $\mathrm{SU}(2)_L$, $\mathrm{SU}(2)_R$, and $\mathrm{SU}(4)_C$, respectively.

APPENDIX C: ONE-LOOP FORMULAS FOR GAUGE COUPLING UNIFICATION

At the one-loop level, the gauge coupling RGEs are easily solved analytically. By using the solutions, we can obtain analytic expressions for $M_{\rm int}$, $M_{\rm GUT}$, and $\alpha_{\rm GUT}$ as follows:

$$M_{\rm int} = m_Z \exp\left[\frac{2\pi(\tilde{\boldsymbol{b}} \times \boldsymbol{n}) \cdot \boldsymbol{\alpha}_{-1}}{(\tilde{\boldsymbol{b}} \times \boldsymbol{n}) \cdot \boldsymbol{b}}\right], \tag{C1}$$

$$M_{\rm GUT} = m_Z \exp\left[\frac{2\pi(\Delta\boldsymbol{b} \times \boldsymbol{n}) \cdot \boldsymbol{\alpha}_{-1}}{(\tilde{\boldsymbol{b}} \times \boldsymbol{n}) \cdot \boldsymbol{b}}\right], \tag{C2}$$

$$\alpha_{\rm GUT}^{-1} = \frac{(\tilde{\boldsymbol{b}} \times \boldsymbol{\alpha}_{-1}) \cdot \boldsymbol{b}}{(\tilde{\boldsymbol{b}} \times \boldsymbol{n}) \cdot \boldsymbol{b}}, \tag{C3}$$

with

$$\boldsymbol{\alpha}_{-1} \equiv \begin{pmatrix} \alpha_1^{-1}(m_Z) \\ \alpha_2^{-1}(m_Z) \\ \alpha_3^{-1}(m_Z) \end{pmatrix}, \qquad \boldsymbol{b} \equiv \begin{pmatrix} b_1 \\ b_2 \\ b_3 \end{pmatrix},$$
$$\tilde{\boldsymbol{b}} \equiv \begin{pmatrix} \tilde{b}_1 \\ \tilde{b}_2 \\ \tilde{b}_3 \end{pmatrix}, \qquad \boldsymbol{n} \equiv \begin{pmatrix} 1 \\ 1 \\ 1 \end{pmatrix}, \tag{C4}$$

where $\Delta\boldsymbol{b} \equiv \tilde{\boldsymbol{b}} - \boldsymbol{b}$, and b_a and $\tilde{b}_a$ denote the beta-function coefficients below and above the intermediate scale, respectively. The U(1) beta function above the intermediate scale is given by a linear combination of the beta functions of the intermediate gauge group. For instance, in the case of $\mathrm{SU}(4)_C \otimes \mathrm{SU}(2)_L \otimes \mathrm{SU}(2)_R$, we have

$$\tilde{b}_1 = \frac{2}{5}b_4 + \frac{3}{5}b_{2R}. \tag{C5}$$

Similar expressions are obtained for other intermediate groups. Notice that the components of the beta-function coefficients which are proportional to $\boldsymbol{n}$ do not affect $M_{\rm GUT}$ and $M_{\rm int}$, as one can see from the formulas. Therefore, if one adds a multiplet to, e.g., the

$SU(4)_C\otimes SU(2)_L\otimes SU(2)_R$ theory whose contribution to the beta-function coefficients is $\Delta b_4=\Delta b_{2L}=\Delta b_{2R}$, then the multiplet does not alter $M_{\rm GUT}$ and $M_{\rm int}$ at the one-loop level.

We also note that physics above the intermediate scale gives negligible effects on the determination of $M_{\rm int}$ in the presence of the left-right symmetry. We can see this feature by using Eq. (C1). Let us consider the case of $SU(4)_C\otimes SU(2)_L\otimes SU(2)_R\otimes D$. In the left-right-symmetric theories, the beta functions of the $SU(2)_L$ and $SU(2)_R$ gauge couplings should be the same. Therefore, we have $b_{2L}=b_{2R}$, and

$$\tilde{\boldsymbol{b}}\times\boldsymbol{n}=(b_{2L}-b_4)\boldsymbol{c}, \tag{C6}$$

with

$$\boldsymbol{c}=\begin{pmatrix}1\\-\frac{3}{5}\\-\frac{2}{5}\end{pmatrix}. \tag{C7}$$

Therefore, Eq. (C1) reads

$$M_{\rm int}=m_Z\exp\left[\frac{2\pi\boldsymbol{c}\cdot\boldsymbol{\alpha_{-1}}}{\boldsymbol{c}\cdot\boldsymbol{b}}\right], \tag{C8}$$

and thus, the intermediate scale does not depend on the beta function above $M_{\rm int}$. One can also see this feature by noting that above the intermediate scale $g_{2L}=g_{2R}$ holds at any scale. Hence, the intermediate scale corresponds to a point at which g_{2L} becomes equivalent to g_{2R}, which is determined only by the running below $M_{\rm int}$. A similar argument holds in the case of $SU(3)_C\otimes SU(2)_L\otimes SU(2)_R\otimes U(1)_{B-L}\otimes D$.

APPENDIX D: PROTON DECAY IN $\mathbf{SO(10)\to SU(4)\otimes SU(2)\otimes SU(2)}$

Here, we give details of the calculation for the proton decay lifetime in the intermediate-scale scenario. We consider the case of $SO(10)\to SU(4)\otimes SU(2)\otimes SU(2)$, which was discussed in Sec. V B.

In non-SUSY GUTs, proton decay is induced by gauge interactions. The relevant interactions are written as

$$\begin{aligned}\mathcal{L}_{\rm int}=\frac{g_{\rm GUT}}{\sqrt{2}}&[(\bar{Q})_{ar}\not{X}^{air}P_R(L^{\mathcal{C}})_i+(\bar{Q})_{ai}\not{X}^{air}P_L(L^{\mathcal{C}})_r\\&+\epsilon_{ij}\epsilon_{rs}\epsilon_{abc}(\overline{Q^{\mathcal{C}}})^{ar}\not{X}^{bis}P_LQ^{cj}+\text{H.c.}],\end{aligned} \tag{D1}$$

where

$$Q=\begin{pmatrix}u\\d\end{pmatrix},\qquad L=\begin{pmatrix}\nu\\e^-\end{pmatrix}, \tag{D2}$$

and X denotes the superheavy gauge bosons which induce the baryon-number-violating interactions; $g_{\rm GUT}$ is the unified gauge coupling constant; a,b,c, i,j, and r,s are the $SU(3)_C$, $SU(2)_L$, and $SU(2)_R$ indices, respectively, and; $P_{R/L}\equiv(1\pm\gamma_5)/2$ are the chirality projection operators.

After integrating out the SO(10) gauge fields X, we obtain the dimension-six proton decay operator. The operator is expressed in a form that respects the intermediate gauge symmetry, $SU(4)\otimes SU(2)\otimes SU(2)$:

$$\mathcal{L}_{\rm eff}=C(M_{\rm GUT})\cdot\epsilon_{ij}\epsilon_{rs}\epsilon_{\alpha\beta\gamma\delta}(\overline{\Psi^{\mathcal{C}}})^{\alpha i}P_L\Psi^{\beta j}(\overline{\Psi^{\mathcal{C}}})^{\gamma r}P_R\Psi^{\delta s}, \tag{D3}$$

where $\alpha,\beta,\ldots$ denote the SU(4) indices, and Ψ is given in Eq. (13). Notice that

$$\begin{aligned}&\epsilon_{ij}\epsilon_{kl}\epsilon_{\alpha\beta\gamma\delta}(\overline{\Psi^{\mathcal{C}}})^{\alpha i}P_L\Psi^{\beta j}(\overline{\Psi^{\mathcal{C}}})^{\gamma k}P_L\Psi^{\delta l}\\&\quad=\epsilon_{rs}\epsilon_{tu}\epsilon_{\alpha\beta\gamma\delta}(\overline{\Psi^{\mathcal{C}}})^{\alpha r}P_R\Psi^{\beta s}(\overline{\Psi^{\mathcal{C}}})^{\gamma t}P_R\Psi^{\delta u}=0,\end{aligned} \tag{D4}$$

and thus the operator in Eq. (D3) is the unique choice. At tree level, the coefficient of the effective operator is evaluated as

$$C(M_{\rm GUT})=\frac{g_{\rm GUT}^2}{2M_X^2}, \tag{D5}$$

with M_X the mass of the heavy gauge field X. Here, we have neglected fermion flavor mixings [51] for simplicity.

The Wilson coefficient is evolved down to the intermediate scale using the RGE. The renormalization factor is computed to be [52]

$$\begin{aligned}C(M_{\rm int})=&\left[\frac{\alpha_4(M_{\rm int})}{\alpha_{\rm GUT}}\right]^{-\frac{15}{4b_4}}\left[\frac{\alpha_{2L}(M_{\rm int})}{\alpha_{\rm GUT}}\right]^{-\frac{9}{4b_{2L}}}\\&\times\left[\frac{\alpha_{2R}(M_{\rm int})}{\alpha_{\rm GUT}}\right]^{-\frac{9}{4b_{2R}}}C(M_{\rm GUT}).\end{aligned} \tag{D6}$$

At the intermediate scale, the $SU(4)\otimes SU(2)\otimes SU(2)$ theory is matched onto the SM. The effective Lagrangian is written as

$$\mathcal{L}_{\rm eff}=\sum_{I=1}^{4}C_I\mathcal{O}_I, \tag{D7}$$

with the effective operators given by [53–55]

$$\begin{aligned}\mathcal{O}_1&=\epsilon_{abc}\epsilon_{ij}(u_R^ad_R^b)(Q_L^{ci}L_L^j),\\\mathcal{O}_2&=\epsilon_{abc}\epsilon_{ij}(Q_L^{ai}Q_L^{bj})(u_R^ce_R),\\\mathcal{O}_3&=\epsilon_{abc}\epsilon_{ij}\epsilon_{kl}(Q_L^{ai}Q_L^{bk})(Q_L^{cl}L_L^j),\\\mathcal{O}_4&=\epsilon_{abc}(u_R^ad_R^b)(u_R^ce_R).\end{aligned} \tag{D8}$$

We evaluate the coefficients C_I as

$$C_1(M_{\rm int}) = 4C(M_{\rm int}),$$
$$C_2(M_{\rm int}) = -4C(M_{\rm int}),$$
$$C_3(M_{\rm int}) = C_4(M_{\rm int}) = 0. \tag{D9}$$

We then run down the coefficients to the electroweak scale. The renormalization factors are given by [55]

$$C_1(m_Z) = \left[\frac{\alpha_3(m_Z)}{\alpha_3(M_{\rm int})}\right]^{-\frac{2}{b_3}}\left[\frac{\alpha_2(m_Z)}{\alpha_2(M_{\rm int})}\right]^{-\frac{9}{4b_2}} \times \left[\frac{\alpha_1(m_Z)}{\alpha_1(M_{\rm int})}\right]^{-\frac{11}{20b_1}} C_1(M_{\rm int}), \tag{D10}$$

$$C_2(m_Z) = \left[\frac{\alpha_3(m_Z)}{\alpha_3(M_{\rm int})}\right]^{-\frac{2}{b_3}}\left[\frac{\alpha_2(m_Z)}{\alpha_2(M_{\rm int})}\right]^{-\frac{9}{4b_2}} \times \left[\frac{\alpha_1(m_Z)}{\alpha_1(M_{\rm int})}\right]^{-\frac{23}{20b_1}} C_2(M_{\rm int}). \tag{D11}$$

Note that the beta-function coefficients should be appropriately modified when the number of quark flavors changes. Below the electroweak scale, the QCD corrections are the dominant contribution. By using the two-loop RGE given in Ref. [56], we compute the Wilson coefficients at the hadronic scale $\mu_{\rm had}$ as

$$C_i(\mu_{\rm had}) = \left[\frac{\alpha_s(\mu_{\rm had})}{\alpha_s(m_b)}\right]^{\frac{6}{25}}\left[\frac{\alpha_s(m_b)}{\alpha_s(m_Z)}\right]^{\frac{6}{23}}\left[\frac{\alpha_s(\mu_{\rm had})+\frac{50\pi}{77}}{\alpha_s(m_b)+\frac{50\pi}{77}}\right]^{-\frac{173}{825}} \times \left[\frac{\alpha_s(m_b)+\frac{23\pi}{29}}{\alpha_s(m_Z)+\frac{23\pi}{29}}\right]^{-\frac{430}{2001}} C_i(m_Z), \tag{D12}$$

with $i = 1, 2$.

In non-SUSY GUTs, the dominant decay mode of proton is $p \to \pi^0 e^+$. The partial decay width of the mode is computed as

$$\Gamma(p \to \pi^0 e^+) = \frac{m_p}{32\pi}\left(1 - \frac{m_\pi^2}{m_p^2}\right)^2 [|\mathcal{A}_L|^2 + |\mathcal{A}_R|^2], \tag{D13}$$

where m_p and m_π are the masses of the proton and the neutral pion, respectively, and

$$\mathcal{A}_L = C_1(\mu_{\rm had})\langle\pi^0|(ud)_R u_L|p\rangle,$$
$$\mathcal{A}_R = 2C_2(\mu_{\rm had})\langle\pi^0|(ud)_L u_R|p\rangle. \tag{D14}$$

The hadron matrix elements are evaluated with the lattice QCD simulations in Ref. [57]. We have

$$\langle\pi^0|(ud)_R u_L|p\rangle = \langle\pi^0|(ud)_L u_R|p\rangle = -0.103(23)(34)\ \text{GeV}^2, \tag{D15}$$

with $\mu_{\rm had} = 2$ GeV. Here, the first and second parentheses indicate statistical and systematic errors, respectively.

[1] J. R. Ellis, S. Kelley, and D. V. Nanopoulos, Precision LEP data, supersymmetric GUTs and string unification, Phys. Lett. B **249**, 441 (1990); Probing the desert using gauge coupling unification, Phys. Lett. B **260**, 131 (1991); U. Amaldi, W. de Boer, and H. Furstenau, Comparison of grand unified theories with electroweak and strong coupling constants measured at LEP, Phys. Lett. B **260**, 447 (1991); C. Giunti, C. W. Kim, and U. W. Lee, Running coupling constants and grand unification models, Mod. Phys. Lett. A **06**, 1745 (1991); P. Langacker and M. x. Luo, Implications of precision electroweak experiments for M_t, ρ_0, $\sin^2\theta_W$ and grand unification, Phys. Rev. D **44**, 817 (1991).

[2] S. Rajpoot, Symmetry breaking and intermediate mass scales in the SO(10) grand unified theory, Phys. Rev. D **22**, 2244 (1980); M. Yasue, Phenomenological aspect of SO(10) grand unified model, Prog. Theor. Phys. **65**, 708 (1981); **65**, 1480(E) (1981); J. M. Gipson and R. E. Marshak, Intermediate mass scales in the new SO(10) grand unification in the one loop approximation, Phys. Rev. D **31**, 1705 (1985); D. Chang, R. N. Mohapatra, J. Gipson, R. E. Marshak, and M. K. Parida, Experimental tests of new SO(10) grand unification, Phys. Rev. D **31**, 1718 (1985); N. G. Deshpande, E. Keith, and P. B. Pal, Implications of LEP results for SO(10) grand unification, Phys. Rev. D **46**, 2261 (1992); N. G. Deshpande, E. Keith, and P. B. Pal, Implications of LEP results for SO(10) grand unification with two intermediate stages, Phys. Rev. D **47**, 2892 (1993); S. Bertolini, L. Di Luzio, and M. Malinsky, On the vacuum of the minimal nonsupersymmetric SO(10) unification, Phys. Rev. D **81**, 035015 (2010).

[3] M. Fukugita and T. Yanagida, Physics of neutrinos, in *Physics and Astrophysics of Neutrinos*, edited by M. Fukugita and A. Suzuki (Springer, New York, 1994), pp. 1–248 [Kyoto University Report No. YITP-K-1050 (1994)].

[4] Y. Mambrini, K. A. Olive, J. Quevillon, and B. Zaldivar, Gauge Coupling Unification and Nonequilibrium Thermal Dark Matter, Phys. Rev. Lett. **110**, 241306 (2013).

[5] H. Goldberg, Constraint on the Photino Mass from Cosmology, Phys. Rev. Lett. **50**, 1419 (1983); **103**, 099905 (2009); J. Ellis, J. S. Hagelin, D. V. Nanopoulos, K. A. Olive, and M. Srednicki, Supersymmetric relics from the big bang, Nucl. Phys. **B238**, 453 (1984).

[6] T. W. B. Kibble, G. Lazarides, and Q. Shafi, Strings in SO(10), Phys. Lett. **113B**, 237 (1982).

[7] L. M. Krauss and F. Wilczek, Discrete Gauge Symmetry in Continuum Theories, Phys. Rev. Lett. **62**, 1221 (1989).

[8] L. E. Ibanez and G. G. Ross, Discrete gauge symmetry anomalies, Phys. Lett. B **260**, 291 (1991); Discrete gauge symmetries and the origin of baryon and lepton number conservation in supersymmetric versions of the standard model, Nucl. Phys. **B368**, 3 (1992).

[9] S. P. Martin, Some simple criteria for gauged R-parity, Phys. Rev. D **46**, R2769 (1992).

[10] M. Kadastik, K. Kannike, and M. Raidal, Matter parity as the origin of scalar dark matter, Phys. Rev. D **81**, 015002 (2010). Dark matter as the signal of grand unification, Phys. Rev. D **80**, 085020 (2009); **81**, 029903(E) (2010).

[11] M. Frigerio and T. Hambye, Dark matter stability and unification without supersymmetry, Phys. Rev. D **81**, 075002 (2010); T. Hambye, On the stability of particle dark matter, *Proc. Sci.*, IDM2010 (2011) 098.

[12] L. J. Hall, K. Jedamzik, J. March-Russell, and S. M. West, Freeze-in production of FIMP dark matter, J. High Energy Phys. 03 (2010) 080; J. McDonald, Thermally Generated Gauge Singlet Scalars as Self-Interacting Dark Matter, Phys. Rev. Lett. **88**, 091304 (2002); X. Chu, T. Hambye, and M. H. G. Tytgat, The four basic ways of creating dark matter through a portal, J. Cosmol. Astropart. Phys. 05 (2012) 034; C. E. Yaguna, An intermediate framework between WIMP, FIMP, and EWIP dark matter, J. Cosmol. Astropart. Phys. 02 (2012) 006.

[13] M. De Montigny and M. Masip, Discrete gauge symmetries in supersymmetric grand unified models, Phys. Rev. D **49**, 3734 (1994).

[14] E. B. Dynkin, Transl.-Am. Math. Soc. **6**, 111 (1957); E. Dynkin, *Selected Papers of EB Dynkin with Commentary* (American Mathematical Society, Providence, RI, 2000), p. 37.

[15] R. Slansky, Group theory for unified model building, Phys. Rep. **79**, 1 (1981).

[16] H. Georgi, Lie algebras in particle physics: From isospin to unified theories, Front. Phys. **54**, 1 (1982).

[17] S. M. Barr, A new symmetry breaking pattern for SO(10) and proton decay, Phys. Lett. **112B**, 219 (1982); Some comments on flipped $\mathbf{SU}(5) \times \boldsymbol{U}(1)$ and flipped unification in general, Phys. Rev. D **40**, 2457 (1989); J. P. Derendinger, J. E. Kim, and D. V. Nanopoulos, Anti-SU(5), Phys. Lett. **139B**, 170 (1984).

[18] I. Antoniadis, J. R. Ellis, J. S. Hagelin, and D. V. Nanopoulos, Supersymmetric flipped SU(5) revitalized, Phys. Lett. B **194**, 231 (1987).

[19] G. R. Farrar and P. Fayet, Phenomenology of the production, decay, and detection of new hadronic states associated with supersymmetry, Phys. Lett. **76B**, 575 (1978); S. Dimopoulos and H. Georgi, Softly broken supersymmetry and SU(5), Nucl. Phys. **B193**, 150 (1981); S. Weinberg, Supersymmetry at ordinary energies: 1. Masses and conservation laws, Phys. Rev. D **26**, 287 (1982); N. Sakai and T. Yanagida, Proton decay in a class of supersymmetric grand unified models, Nucl. Phys. **B197**, 533 (1982); S. Dimopoulos, S. Raby, and F. Wilczek, Proton decay in supersymmetric models, Phys. Lett. **112B**, 133 (1982).

[20] V. A. Kuzmin and M. E. Shaposhnikov, Baryon asymmetry of the Universe versus left-right symmetry, Phys. Lett. **92B**, 115 (1980); T. W. B. Kibble, G. Lazarides, and Q. Shafi, Walls bounded by strings, Phys. Rev. D **26**, 435 (1982); D. Chang, R. N. Mohapatra, and M. K. Parida, Decoupling Parity and SU(2)-R Breaking Scales: A New Approach to Left-Right Symmetric Models, Phys. Rev. Lett. **52**, 1072 (1984); D. Chang, R. N. Mohapatra, and M. K. Parida, A new approach to left-right symmetry breaking in unified gauge theories, Phys. Rev. D **30**, 1052 (1984); D. Chang, R. N. Mohapatra, J. Gipson, R. E. Marshak, and M. K. Parida, Experimental tests of new SO(10) grand unification, Phys. Rev. D **31**, 1718 (1985).

[21] P. F. Smith and J. R. J. Bennett, A search for heavy stable particles, Nucl. Phys. **B149**, 525 (1979); P. F. Smith, J. R. J. Bennett, G. J. Homer, J. D. Lewin, H. E. Walford, and W. A. Smith, A search for anomalous hydrogen in enriched D-2 O, using a time-of-flight spectrometer, Nucl. Phys. **B206**, 333 (1982); T. K. Hemmick, D. Elmore, T. Gentile, P. W. Kubik, S. L. Olsen, D. Ciampa, D. Nitz, H. Kagan *et al.*, A search for anomalously heavy isotopes of low $\boldsymbol{Z}$ nuclei, Phys. Rev. D **41**, 2074 (1990); P. Verkerk, G. Grynberg, B. Pichard, M. Spiro, S. Zylberajch, M. E. Goldberg, and P. Fayet, Search for Superheavy Hydrogen in Sea Water, Phys. Rev. Lett. **68**, 1116 (1992); T. Yamagata, Y. Takamori, and H. Utsunomiya, Search for anomalously heavy hydrogen in deep sea water at 4000 m, Phys. Rev. D **47**, 1231 (1993).

[22] L. Di Luzio, Aspects of symmetry breaking in grand unified theories, arXiv:1110.3210.

[23] F. del Aguila and L. E. Ibanez, Higgs bosons in SO(10) and partial unification, Nucl. Phys. **B177**, 60 (1981).

[24] R. N. Mohapatra and G. Senjanovic, Higgs Boson effects in grand unified theories, Phys. Rev. D **27**, 1601 (1983).

[25] P. Minkowski, $\mu \to e\gamma$ at a rate of one out of 1-billion muon decays?, Phys. Lett. **67B**, 421 (1977); T. Yanagida, Horizontal symmetry and masses of neutrinos, Conf. Proc. C **7902131**, 95 (1979); M. Gell-Mann, P. Ramond, and R. Slansky, Complex spinors and unified theories, Conf. Proc. C **790927**, 315 (1979); S. L. Glashow, The future of elementary particle physics, NATO Sci. Ser. B **59**, 687 (1980); R. N. Mohapatra and G. Senjanovic, Neutrino Mass and Spontaneous Parity Violation, Phys. Rev. Lett. **44**, 912 (1980).

[26] I. Antoniadis, J. R. Ellis, J. S. Hagelin, and D. V. Nanopoulos, An improved $\mathrm{SU}(5) \times \mathrm{U}(1)$ model from four-dimensional string, Phys. Lett. B **208**, 209 (1988); **213**, 562(E) (1988); J. R. Ellis, J. L. Lopez, and D. V. Nanopoulos, The prospects for CHORUS and NOMAD in the light of COBE and GALLEX, Phys. Lett. B **292**, 189 (1992); J. R. Ellis, D. V. Nanopoulos, and K. A. Olive, Flipped heavy neutrinos: From the solar neutrino problem to baryogenesis, Phys. Lett. B **300**, 121 (1993); J. R. Ellis, J. L. Lopez, D. V. Nanopoulos, and K. A. Olive, Flipped angles and phases: A systematic study, Phys. Lett. B **308**, 70 (1993).

[27] J. C. Pati and A. Salam, Lepton number as the fourth color, Phys. Rev. D **10**, 275 (1974); **11**, 703(E) (1975).

[28] B. Bajc, A. Melfo, G. Senjanovic, and F. Vissani, Yukawa sector in non-supersymmetric renormalizable SO(10), Phys. Rev. D **73**, 055001 (2006).

[29] T. Fukuyama, A. Ilakovac, T. Kikuchi, S. Meljanac, and N. Okada, General formulation for proton decay rate in minimal supersymmetric SO(10) GUT, Eur. Phys. J. C **42**, 191 (2005).

[30] W. Siegel, Supersymmetric dimensional regularization via dimensional reduction, Phys. Lett. **84B**, 193 (1979).

[31] S. Weinberg, Effective gauge theories, Phys. Lett. **91B**, 51 (1980); L. J. Hall, Grand unification of effective gauge theories, Nucl. Phys. **B178**, 75 (1981).

[32] S. A. R. Ellis and J. D. Wells, Visualizing gauge unification with high-scale thresholds, Phys. Rev. D **91**, 075016 (2015).

[33] T. Fukuyama, A. Ilakovac, T. Kikuchi, S. Meljanac, and N. Okada, SO(10) group theory for the unified model building, J. Math. Phys. (N.Y.) **46**, 033505 (2005).

[34] R. N. Mohapatra and G. Senjanovic, Neutrino masses and mixings in gauge models with spontaneous parity violation, Phys. Rev. D **23**, 165 (1981).

[35] G. Lazarides, Q. Shafi, and C. Wetterich, Proton lifetime and fermion masses in an SO(10) model, Nucl. Phys. **B181**, 287 (1981).

[36] K. S. Babu and R. N. Mohapatra, Predictive Neutrino Spectrum in Minimal SO(10) Grand Unification, Phys. Rev. Lett. **70**, 2845 (1993).

[37] K. Matsuda, Y. Koide, and T. Fukuyama, Can the SO(10) model with two Higgs doublets reproduce the observed fermion masses? Phys. Rev. D **64**, 053015 (2001).

[38] N. Sakai and T. Yanagida, Proton decay in a class of supersymmetric grand unified models, Nucl. Phys. **B197**, 533 (1982); S. Weinberg, Supersymmetry at ordinary energies: 1. Masses and conservation laws, Phys. Rev. D **26**, 287 (1982).

[39] M. Liu and P. Nath, Higgs boson mass, proton decay, naturalness, and constraints of the LHC and Planck data, Phys. Rev. D **87**, 095012 (2013); J. Hisano, T. Kuwahara, and N. Nagata, Grand unification in high-scale supersymmetry, Phys. Lett. B **723**, 324 (2013); J. Hisano, D. Kobayashi, T. Kuwahara, and N. Nagata, Decoupling can revive minimal supersymmetric SU(5), J. High Energy Phys. 07 (2013) 038; J. Hisano, D. Kobayashi, and N. Nagata, Enhancement of proton decay rates in supersymmetric SU(5) grand unified models, Phys. Lett. B **716**, 406 (2012); N. Yamatsu, A supersymmetric grand unified model with noncompact horizontal symmetry, Prog. Theor. Exp. Phys. **2013**, 123B01 (2013); M. Dine, P. Draper, and W. Shepherd, Proton decay at M_{pl} and the scale of SUSY-breaking, J. High Energy Phys. 02 (2014) 027; L. Du, X. Li, and D. X. Zhang, Proton decay in a supersymmetric SO(10) model with missing partner mechanism, J. High Energy Phys. 04 (2014) 027; N. Nagata and S. Shirai, Sfermion flavor and proton decay in high-scale supersymmetry, J. High Energy Phys. 03 (2014) 049; L. J. Hall, Y. Nomura, and S. Shirai, Grand unification, axion, and inflation in intermediate scale supersymmetry, J. High Energy Phys. 06 (2014) 137; A. Hebecker and J. Unwin, Precision unification and proton decay in F-Theory GUTs with high scale supersymmetry, J. High Energy Phys. 09 (2014) 125; J. L. Evans, N. Nagata, and K. A. Olive, SU(5) grand unification in pure gravity mediation, Phys. Rev. D **91**, 055027 (2015).

[40] M. Shiozawa, Talk presented at TAUP 2013, 8–13 September 2013, Asilomar, CA, USA.

[41] K. S. Babu, E. Kearns, U. Al-Binni, S. Banerjee, D. V. Baxter, Z. Berezhiani, M. Bergevin, S. Bhattacharya *et al.*, Working group report: Baryon number violation, arXiv:1311.5285.

[42] K. Abe, T. Abe, H. Aihara, Y. Fukuda, Y. Hayato, K. Huang, A. K. Ichikawa, M. Ikeda *et al.*, Letter of intent: The Hyper-Kamiokande experiment—Detector design and physics potential, arXiv:1109.3262.

[43] M. Fukugita and T. Yanagida, Baryogenesis without grand unification, Phys. Lett. B **174**, 45 (1986).

[44] G. Lazarides and Q. Shafi, Origin of matter in the inflationary cosmology, Phys. Lett. B **258**, 305 (1991).

[45] K. A. Olive *et al.* (Particle Data Group), Review of particle physics, Chin. Phys. C **38**, 090001 (2014).

[46] ATLAS, CDF, CMS, and D0 Collaborations, First combination of Tevatron and LHC measurements of the top-quark mass, arXiv:1403.4427.

[47] CMS Collaboration, Updated measurements of the Higgs boson at 125 GeV in the two photon decay channel, Report No. CMS-PAS-HIG-13-001; ATLAS Collaboration, Measurements of the properties of the Higgs-like boson in the two photon decay channel with the ATLAS detector using 25 fb^{-1} of proton-proton collision data, Reports No. ATLAS-CONF-2013-012 and No. ATLAS-COM-CONF-2013-015; G. Aad *et al.* (ATLAS Collaboration), Measurements of Higgs boson production and couplings in diboson final states with the ATLAS detector at the LHC, Phys. Lett. B **726**, 88 (2013); **734**, 406(E) (2014); P. P. Giardino, K. Kannike, I. Masina, M. Raidal, and A. Strumia, The universal Higgs fit, J. High Energy Phys. 05 (2014) 046.

[48] Y. Yamada, Two loop renormalization of gaugino mass in supersymmetric gauge model, Phys. Lett. B **316**, 109 (1993).

[49] M. E. Machacek and M. T. Vaughn, Two loop renormalization group equations in a general quantum field theory: 1. Wave function renormalization, Nucl. Phys. **B222**, 83 (1983).

[50] F. Lyonnet, I. Schienbein, F. Staub, and A. Wingerter, PyR@TE: Renormalization group equations for general gauge theories, Comput. Phys. Commun. **185**, 1130 (2014).

[51] P. Fileviez Perez, Fermion mixings versus $d = 6$ proton decay, Phys. Lett. B **595**, 476 (2004).

[52] C. Munoz, Enhancement factors for supersymmetric proton decay in SU(5) and SO(10) with superfield techniques, Phys. Lett. B **177**, 55 (1986).

[53] S. Weinberg, Baryon and Lepton Nonconserving Processes, Phys. Rev. Lett. **43**, 1566 (1979).

[54] F. Wilczek and A. Zee, Operator Analysis of Nucleon Decay, Phys. Rev. Lett. **43**, 1571 (1979).

[55] L. F. Abbott and M. B. Wise, The effective Hamiltonian for nucleon decay, Phys. Rev. D **22**, 2208 (1980).

[56] T. Nihei and J. Arafune, The two loop long range effect on the proton decay effective Lagrangian, Prog. Theor. Phys. **93**, 665 (1995).

[57] Y. Aoki, E. Shintani, and A. Soni, Proton decay matrix elements on the lattice, Phys. Rev. D **89**, 014505 (2014).